Since January 2020 Elsevier has created a COVID-19 resource centre with free information in English and Mandarin on the novel coronavirus COVID-19. The COVID-19 resource centre is hosted on Elsevier Connect, the company's public news and information website.

Infection, Genetics and Evolution 104 (2022) 105355

Contents lists available at ScienceDirect

Infection, Genetics and Evolution

journal homepage: www.elsevier.com/locate/meegid

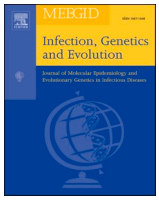

Insight into the first multi-epitope-based peptide subunit vaccine against avian influenza A virus (H5N6): An immunoinformatics approach

Md. Mukthar Mia [a,b], Mahamudul Hasan [b,*], Shakil Ahmed [b], Mohammad Nahian Rahman [b]

[a] Department of Poultry Science, Faculty of Veterinary, Animal and Biomedical Sciences, Sylhet Agricultural University, Sylhet 3100, Bangladesh
[b] Faculty of Veterinary, Animal and Biomedical Sciences, Sylhet Agricultural University, Sylhet 3100, Bangladesh

ARTICLE INFO

Keywords:
Molecular docking
Epitopes
In-silico cloning
Codon optimization
Molecular dynamics simulations
Avian influenza A (H5N6) viruses

ABSTRACT

The rampant spread of highly pathogenic avian influenza A (H5N6) virus has drawn additional concerns along with ongoing Covid-19 pandemic. Due to its migration-related diffusion, the situation is deteriorating. Without an existing effective therapy and vaccines, it will be baffling to take control measures. In this regard, we propose a revers vaccinology approach for prediction and design of a multi-epitope peptide based vaccine. The induction of humoral and cell-mediated immunity seems to be the paramount concern for a peptide vaccine candidate; thus, antigenic B and T cell epitopes were screened from the surface, membrane and envelope proteins of the avian influenza A (H5N6) virus, and passed through several immunological filters to determine the best possible one. Following that, the selected antigenic with immunogenic epitopes and adjuvant were linked to finalize the multi-epitope-based peptide vaccine by appropriate linkers. For the prediction of an effective binding, molecular docking was carried out between the vaccine and immunological receptors (TLR8). Strong binding affinity and good docking scores clarified the stringency of the vaccines. Furthermore, molecular dynamics simulation was performed within the highest binding affinity complex to observe the stability, and minimize the designed vaccine's high mobility region to order to increase its stability. Then, Codon optimization and other physico-chemical properties were performed to reveal that the vaccine would be suitable for a higher expression at cloning level and satisfactory thermostability condition. In conclusion, predicting the overall in silico assessment, we anticipated that our designed vaccine would be a plausible prevention against avian influenza A (H5N6) virus.

1. Introduction

Avian influenza refers to the infection of avian influenza type A virus belonging to the Orthomyxoviridae family which occur naturally among wild aquatic birds, domestic poultry sources of poultry and human population throughout the world (Wu et al., 2017). Humans are not normally affected by avian influenza virus (AIV), but infections can occur via direct contact with infected birds or their excretions, or through limited human to human transmission (Farooqui et al., 2016; Zhang et al., 2015). Previous study reported, human infection with various subtypes of AIV causes severe respiratory disease (Bi et al., 2019), resulting in 3 to 5 million unadorned illnesses and up to 650,000 annual respiratory fatalities globally throughout the world (WHO, 2018). Due to significant improvements in laboratory characterization and surveillance, different novel AIV subtypes are likely to be identified over time. Following the appearance of the H5N1 virus in 1997, ongoing surveillance efforts detected the H7N9 and H10N8 viruses in the last decade a few years ago 2013, causing severe infections in the human population (Wu et al., 2017). In recent years, rapidly emerging H5N6 subtype has supplanted by H5N1 as the most predominant (Highly Pathogenic Avian Influenza Virus) HPAIV, which is currently infecting the humans and other mammals. Sometimes, combined with the enzootic H5N1 and H9N2 strains, this new arrival pathogens create a significant risks to public health (Su et al., 2015; Wen et al., 2021).

The first fatal human infection with the H5N6 virus was associated with the poultry outbreak in China in 2014 (Pan et al., 2016; Yang et al., 2015). In the next year, in 2015, another two outbreaks were documented from Shangrila city of Yunnan province. However, from 2014 to 2021 total 51 AIV-A (H5N6) human infections have been reported including 25 deaths (CDC, 2021) and most infections were found recorded in 2021. In addition, five new cases of AIV-A (H5N6) virus outside of China were documented in the first month of 2022, increasing

* Corresponding author at: Faculty of Veterinary, Animal and Biomedical Sciences, Sylhet Agricultural University, Sylhet 3100, Bangladesh.
E-mail address: mhasan.student@gmail.com (M. Hasan).

https://doi.org/10.1016/j.meegid.2022.105355
Received 9 February 2022; Received in revised form 22 May 2022; Accepted 18 August 2022
Available online 22 August 2022

concerns about the potential of more human infections in the current COVID-19 pandemic.

The pathogenesis of H5N6 subtype may be similar to that of H5N1 infection, with pathological damage in the lungs linked to cytokine dysregulation triggered by H5N6 virus infection and subsequent inflammatory damage to the lungs, diffuse bleeding (De Jong et al., 2006) and damage the liver in conjunction with heart and pneumonia (Hui, 2008; Pan et al., 2016). Therefore, the dearth of efficient therapy and vaccines for humans has worsened the situation.

The genotypes of H5N6 are based on 8 single-stranded RNA segments encoding 11 proteins, including the surface glycoproteins hemagglutinin (HA) and neuraminidase (NA) (Kumar et al., 2018). HA and NA have functions that involve interaction with sialic acid, a terminal structure bound to underlying sugar residues expressed by glycoproteins or

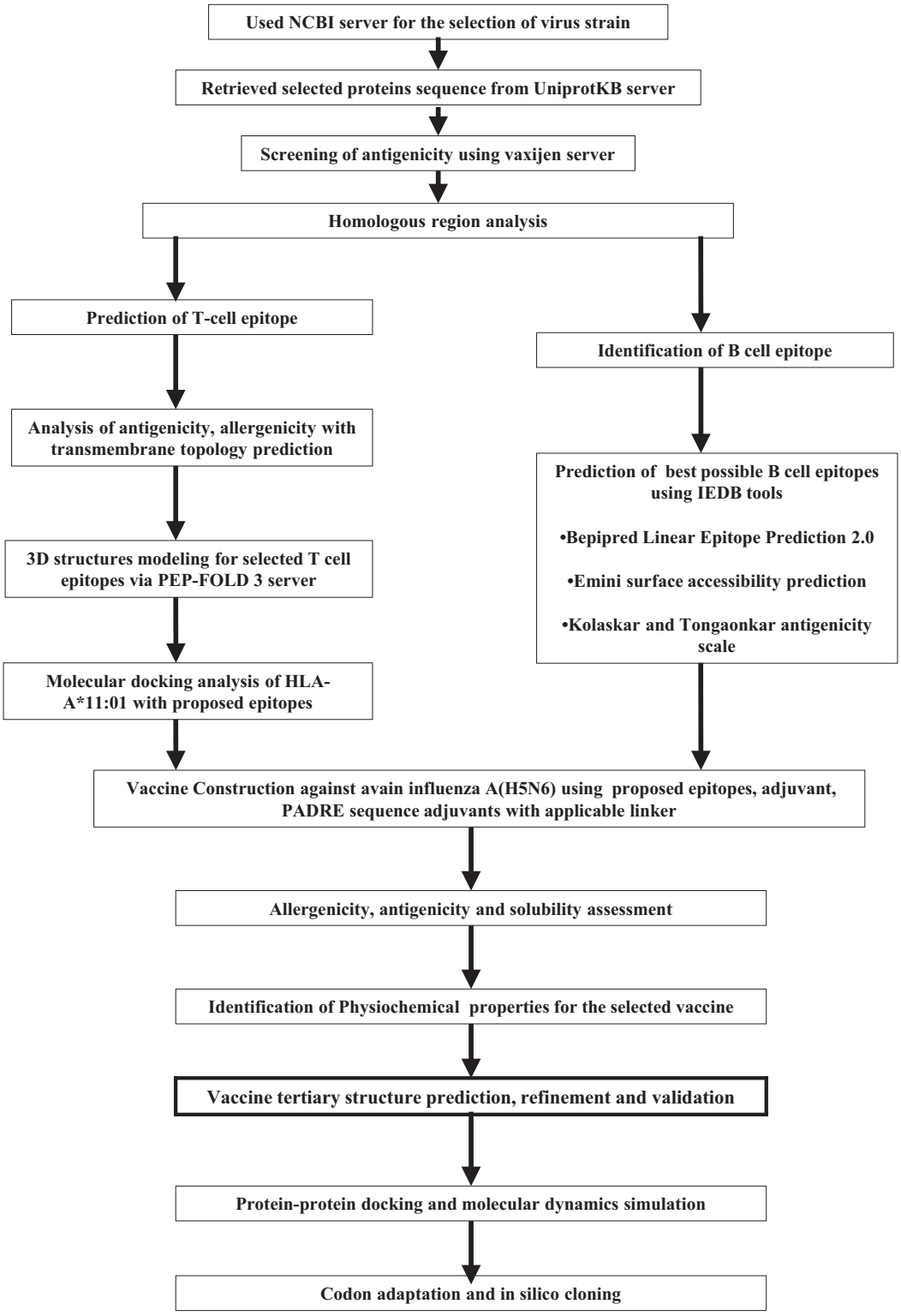

Fig. 1. Flow chart summarized the step-by-step techniques for constructing epitope-based peptide vaccine candidates using computational reverse vaccinology approach.

glycolipids at the cell surface (Cenmidtal and Rosari, 2011). The binding of HA to sialic acids presented by cellular receptors causes cell entry via clathrin-mediated endocytosis, though other endocytic routes, such as micropinocytosis, may also be used (Lakadamyali et al., 2004). NA plays an important role in the final stage of infection. Viral NA removes sialic acids from both cellular receptors as well as newly synthesized HA and NA on nascent virions that have been sialylated as part of the host cell's glycosylation processes (Basak et al., 1985; McAuley et al., 2019). Moreover, NA cleavage of sialic acids prevents virion aggregation and virus binding to the dying host cell via the HA, allowing for efficient virion release and spread to new cell targets (Ilyushina et al., 2012). Because of their vital role in the pathogenicity of the virus, HA and NA have become primary targets in the vaccine design and development fields for neutralizing the AIV (Behbahani et al., 2021; Horimoto and Kawaoka, 2006; Islam et al., 2020). Moreover, previous researches have demonstrated that matrix protein 1 (M1) has a good antibody response (Lohia and Baranwal, 2017; Terajima et al., 2008) and could be the potation target for vaccine construction.

Currently there is no vaccine seed strain capable of eliciting protective immunity against the various clades and subclades of the H5 lineage of HPAIV (Criado et al., 2020). However, previous study reported the possibility of boosting cross-type cellular and humoral immunity against HPAIV subtype H5N1 by vaccination with seasonal influenza A (H1N1)/(H3N2) (Gioia et al., 2008). Regrettably, there is no evidence about the cross reactivity of any existing AIV vaccines including AIV (H5N1) which can protect AIV H5N6 subtype in human. More importantly, H5N6 viruses have been shown to have higher binding affinity to the human receptor and to be more transmissible to contacts than H5N1 viruses (Sun et al., 2016). These findings, together with our findings, show that H5N6 viruses pose a significant threat to public health, despite the small number of human cases (Bi et al., 2016). Therefore, vaccine constructing may facilitate to squeeze the curve of the disease outbreak. Aside from traditional time consuming vaccine design, a recent invention known as reverse vaccinology approach focuses on combining immunogenetics and immunogenomics with bioinformatics to construct unique multi-epitope-based subunit vaccine in a short period of time (Poland et al., 2009). Thus, the current research was intended to generate a non-allergic, immunogenic, and thermostable chimeric vaccine against AIV-A (H5N6) virus employing a vaccinomics methodology and suggested the proposed vaccine candidate's experimental validation in a wet lab with model animals.

2. Materials and methods

The vaccine candidate for AIV-A (H5N6) stain was predicted using a in reverse vaccinology technique. The methodology for developing multi-epitope peptide based vaccines using a reverse vaccinology technique is presented in a flow chart shown in Fig.1.

2.1. Viral strain selection, retrieval of antigenic protein sequences and structure analysis

National Center for Biotechnology Information (NCBI) was used for the selection of avian influenza A (H5N6) strains and analysis of associated information including genus, family, host, transmission, disease, genome and proteome. The UniProtKB database was used to retrieve the full FASTA file of the influenza A (H5N6) strain's viral proteome. While considering the antigenic score over the threshold value, two surface glycoproteins: HA and NA, and M1 of the AIV-A (H5N6) strain were chosen. Following that, the amino acid sequences of the above-listed proteins were inserted into ExPASy's secondary structure prediction program ProtParam server (https://web.expasy.org/protparam/) to predict various physicochemical parameters of the proteins (Gasteiger et al., 2005).

2.2. Conserve regions analysis

NCBI protein BLAST (https://blast.ncbi.nlm.nih.gov/Blast.cgi?PROGRAM=blastp&PAGE_TYPE=BlastSearch&LINK_LOC=blasthome) was used to look for homologous sequences in Influenza A virus (A/Changsha/1/2014(H5N6)) (taxid:1639822), (A/Guangzhou/39715/2014 (H5N6)) (taxid:1612661), and (A/Yunnan/0127/2015(H5N6)) (taxid:1678781), as these serotypes are the most commonly associated with the human infection case. ClustalOmega server (https://www.ebi.ac.uk/Tools/msa/clustalo/) was then applied to specify the conserved regions among the homologous sequences for Hemagglutinin protein (NCBI protein ID: AKC45369.1, AJS18479.1, AKS48023.1), Neuraminidase protein (NCBI protein ID: AKC45371.1, AJS18481.1, AKS48026.1) and Matrix Protein 1 (NCBI protein ID: AKC45372.1, AJS18482.1, AKS48024.1) followed by the use of VaxiJen v2.0 server (http://www.ddg-pharmfac.net/vaxijen/VaxiJen/VaxiJen.html) and TMHMM server (https://services.healthtech.dtu.dk/service.php?TMHMM-2.0) to reveal the antigenicity and topology of the conserved region (Doytchinova and Flower, 2007; Koch et al., 2007). The conserve regions >15 in length, antigenic in nature and outside topology were used to predict T-cell epitopes and linear B cell epitope against each above listed proteins (Supplementary file 1).

2.3. Anticipating of T-cell epitopes and assessment of transmembrane topology, allergenicity and toxicity analysis

MHC class I (HLA A, and B) and II (HLA DR, DP, and DQ) alleles were applied to generate cytotoxic T-cell epitopes (CTL) and helper T-cell (HTL) epitopes, respectively, using the IEDB MHC prediction tools (Lundegaard et al., 2008). The software of the IEDB MHC-I prediction tool was used to assess the analysis of epitopes binding to MHC-I molecules. This server applied artificial neural network (ANN), stabilized matrix method (SMM) or scoring matrices derived from combinatorial peptide libraries (CombLib) to generate the prediction method (Abu-Haraz et al., 2017; Almofti et al., 2018). The length of the epitopes was set to 9 prior to the prediction step. After that, to predict MHC II binding epitopes using the IEDB prediction tool (http://tools.immuneepitope.org/mhcii/), the peptide length was set to 15 amino acids length with the previously mentioned alleles (Verma et al., 2018). In this step, the default IEDB recommended method was applied because this selection tries to use the best possible method for a given MHC molecule using the Consensus approach, combining ANN-align, SMM-align, CombLib, and Sturniolo, if any corresponding predictor is available for the molecule, it uses NetMHCIIpan (http://tools.iedb.org/mhcii/help/#Method).

Following that, the epitopes' antigenic scores and topology were checked using Vaxijen v2.0 server and the TMHMM server, correspondingly. Vaxijen v2.0 server transforms protein sequences using auto cross covariance into uniform vectors of principal amino acid properties and can predict accurate result (Doytchinova and Flower, 2007). Likely, the TMHMM server, based on a hidden Markov model can correctly predict (97–98) % of transmembrane protein topology that makes it unique from other methods. The epitopes FASTA files were loaded into VaxiJen v2.0 sever with setting the threshold value 0.4 and selected the target organism as parasite. In the case of TMHMM server, epitopes FASTA files were loaded into input section and selected the output as extensive with graphics.

Based on the percentile score, higher vaxijen score and topology (outside), the best 20 epitopes were selected. Epitope was considered non-allergenic, which had non-allergenic results from at least three of the servers, including AllergenFP (Dimitrov et al., 2014b), AllerTOP (Dimitrov et al., 2014a), Allermatch (Fiers et al., 2004), and Allergen online (Goodman et al., 2016). Then, ToxinPred server (https://webs.iiitd.edu.in/raghava/toxinpred/multi_submit.php) was used to affirm the toxicity of the selected epitopes (Gupta et al., 2014). This website aims to anticipate epitope toxicity based on all relevant physicochemical properties by using a dataset of 1805 toxic peptides (Zheng et al., 2012).

Epitope's FASTA files were inserted into batch submission input section with keeping the parameters default.

2.4. Population coverage and conservancy analysis

Because HLA genes are distributed differently among ethnic groups and geographical regions around the world, population coverage must be considered while developing a potential vaccination to cover the largest possible population keeping all the parameters default. To investigate the covering population for each epitope, the IEDB server's population coverage analysis tool (http://tools.iedb.org/population/) had been used. This tool is used to calculate the percentage of individuals estimated to respond to a given epitope set based on HLA genotypic frequencies and MHC binding or T cell restriction data (Bui et al., 2006) (Fig. 2). Moreover, the extent of desired epitope distributions in the homologous protein set is specified by epitope conservancy, which is an essential step in the immunoinformatic approach. Thus, the epitope conservancy analysis tool (http://tools.iedb.org/conservancy/) from the IEDB was chosen for assessing the conservancy percentage through focusing on the identities of the protein sequences. The sequence identity threshold was set to 100%, and all other parameters were left at their default values.

2.5. Screening of linear B cell epitopes

The main objective of B cell epitope prediction is to identify a potential antigen that will interact with B lymphocytes and trigger an immunological response. The antigenicity of the peptide is connected to its flexibility, according to the experimental study. Being a possible B cell epitope also necessitates proper surface accessibility. Thus, B cell epitope prediction Tools from IEDB with accuracy of 75%; Sensitivity¼ 0.49 and specificity¼ 0.75 (Saadi et al., 2017; Saha and Raghava, 2006a) was used to identify the B cell antigenicity depending on few algorithms including the Emini surface accessibility prediction, Kolaskar and Tongaonkar antigenicity scale, and Bepipred linear epitope prediction 2.0 (http://tools.iedb.org/bcell/). The Kolaskar and Tongaonkar method is a semi-empirical approach that predicts antigenic determinants on proteins by using the physicochemical properties of amino acid residues and their frequencies of occurrence in experimentally known segmental epitopes (Kolaskar and Tongaonkar, 1990). Meanwhile, Emini surface accessibility prediction was a surface accessibility scale. Likely, BepiPred most likely predicts the location of linear B-cell epitopes by combining a hidden Markov model and a propensity scale method (Emini et al., 1985; Jespersen et al., 2017; Kolaskar and Tongaonkar, 1990) (Fig. 3).

2.6. Construction of vaccine

T-cell epitopes that were superior in terms of global binding energy with human MHC alleles, as well as B-cell epitopes that were low percentile score, more antigenic, non-allergic, non-toxic and overlapped with other epitopes, were used to construct vaccines. Three vaccine candidates (V1, V2, and V3) were created by combining different adjuvants with PADRE sequences and the best (low percentile score, higher vaxijen score, non-toxic, non-allergic and outside topology) HTL epitopes, CTL epitopes, and BCL epitopes. The first vaccination construct employed human defensin adjuvant due to its efficacy as a vaccine adjuvant, whereas the second and third vaccine constructs used ribosomal protein adjuvant and HABA adjuvant due to their efficacy as vaccine adjuvants (Rana and Akhter, 2016). The EAAAK, GGGS, GPGPG, and KK linker were used to connect all of the epitopes and adjuvants because it keeps the domains equal.

2.7. Antigenicity, allergenicity and solubility of the designed vaccine constructs

The non-allergic activity of the developed vaccine was assessed using the AlgPred v.2.0 (Saha and Raghava, 2006b) and AllerTOP v.2.0 (Hebditch et al., 2017) (Dimitrov et al., 2014a) servers. The antigenically superior vaccine candidate was then selected using the VaxiJen v2.0 server (Doytchinova and Flower, 2007). After that, the solubility of the recommended vaccine candidate was determined using Protein-sol server (https://protein-sol.manchester.ac.uk/). It is a web server that predicts protein solubility based on the observation of a bimodal distribution of protein solubilities for *E.coli* proteins in cell-free expression, and these measurements report the amount of a protein that is soluble compared to the total amount of that protein, rather than a thermodynamic property (Hebditch et al., 2017).

2.8. Analysis of physicochemical characteristics, secondary and tertiary structure prediction, refinement and validation of constructed vaccine

The ProtParam server (http://expasy.org/cgi-bin/protpraram) was used to functionally characterize the V1 vaccine candidate (Gasteiger et al., 2005). The physicochemical variables measured included molecular weight, aliphatic index, isoelectric pH, hydropathicity, estimated half-life, instability index, and GRAVY values. The PSIPRED v3.3 server (http://globin.bio.warwick.ac.uk/psipred/) has also been used to predict the vaccine protein's beta-sheet, coil structure, and alpha-helix (Fig. 4). PSIPRED is a highly accurate secondary prediction method that incorporates two feed-forward neural networks that analyze PSI-BLAST output and use a stringent cross validation procedure to evaluate performance (Saadi et al., 2017). Moreover, Ramachandran plot analysis (http://mordred.bioc.cam.ac.uk/rapper/rampage.php) was performed to identify the potential errors in selected vaccine construct (Fig. 5). Then, the Raptor X server performed 3D modeling of the designed vaccines depending on the degree of similarity between target protein and available template structure from PDB (Källberg et al., 2014; Peng and Xu, 2011). To increase the accuracy of the predicted 3D modeled structure, refinement was performed using Galaxy WEB (http://galaxy.seoklab.org/cgi-bin/submit.cgi?type=REFINE).

2.9. Disulfide bonds simulation of the selected vaccine candidate and molecular docking

Disulfide engineering is a novel method of creating new disulfide bonds in a protein of interest by changing cysteine residues in the protein structure, leading to increased protein structure stability (Mugunthan and Harish, 2021). As a result, the Disulfide by Design 2 (DbD2) server (http://cptweb.cpt.wayne.edu/DbD2/) was used to identify residue pairs with the potential for mutation and could be used in disulfide engineering (Alizadeh et al., 2022) (Fig. 9).

Molecular docking is a computational approach that predicts the preferred orientation of the ligand to the receptor when they are joined together to form a stable complex (Tabassum et al., 2021). A recent study reported that, docking success rate with each energy parameter set results in 100 ranked models, ClusPro was the best performer than other newly invented HADDOCK, ZDOCK and Lightdock server (Peacock and Chain, 2021). Thus, we used the ClusPro 2.0 server (https://cluspro.org/login.php) to perform molecular docking (Kozakov et al., 2017; Vajda et al., 2017). Initially, the 3D structure of TLR8 in PDB format (PDB ID: 3W3M) was obtained from the protein data bank (RCSB). The ligands attached to the retrieved TLR8 structure were then removed using Discovery studio software. The refined 3D model of the multi-epitope based peptide vaccine and TLR8 was submitted in the ClusPro 2.0 server as ligand and receptor, respectively. Similarly, refined 3D model of the multi-epitope vaccine with different HLA alleles' pdf files (Table 8) were loaded into ClusPro 2.0 as ligand and receptor, individually.

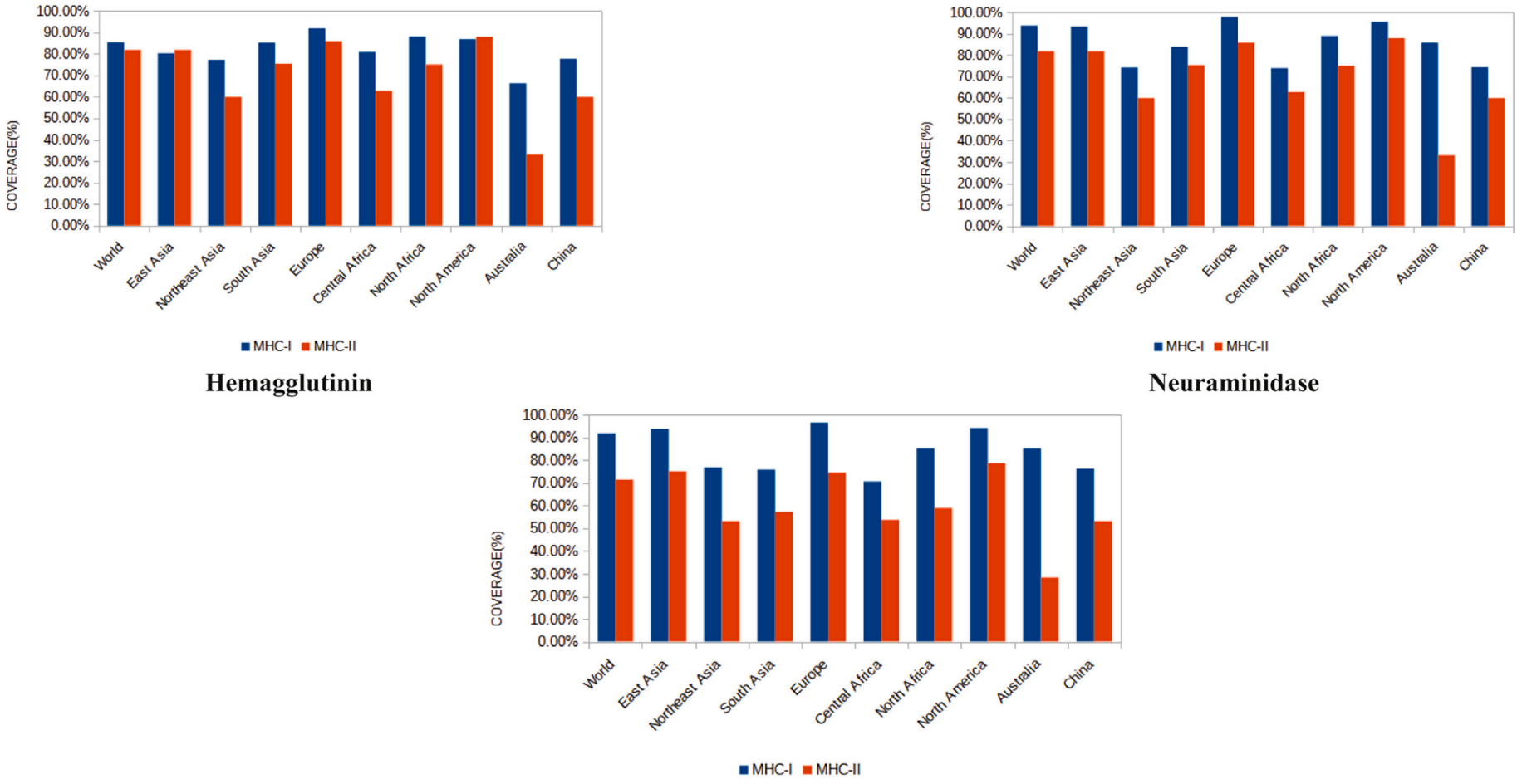

Fig. 2. Population coverage analysis of envelope glycoprotein (Hemagglutinin, Neuraminidase and Matrix Protein 1) around the world prophesied by IEDB population coverage tool.

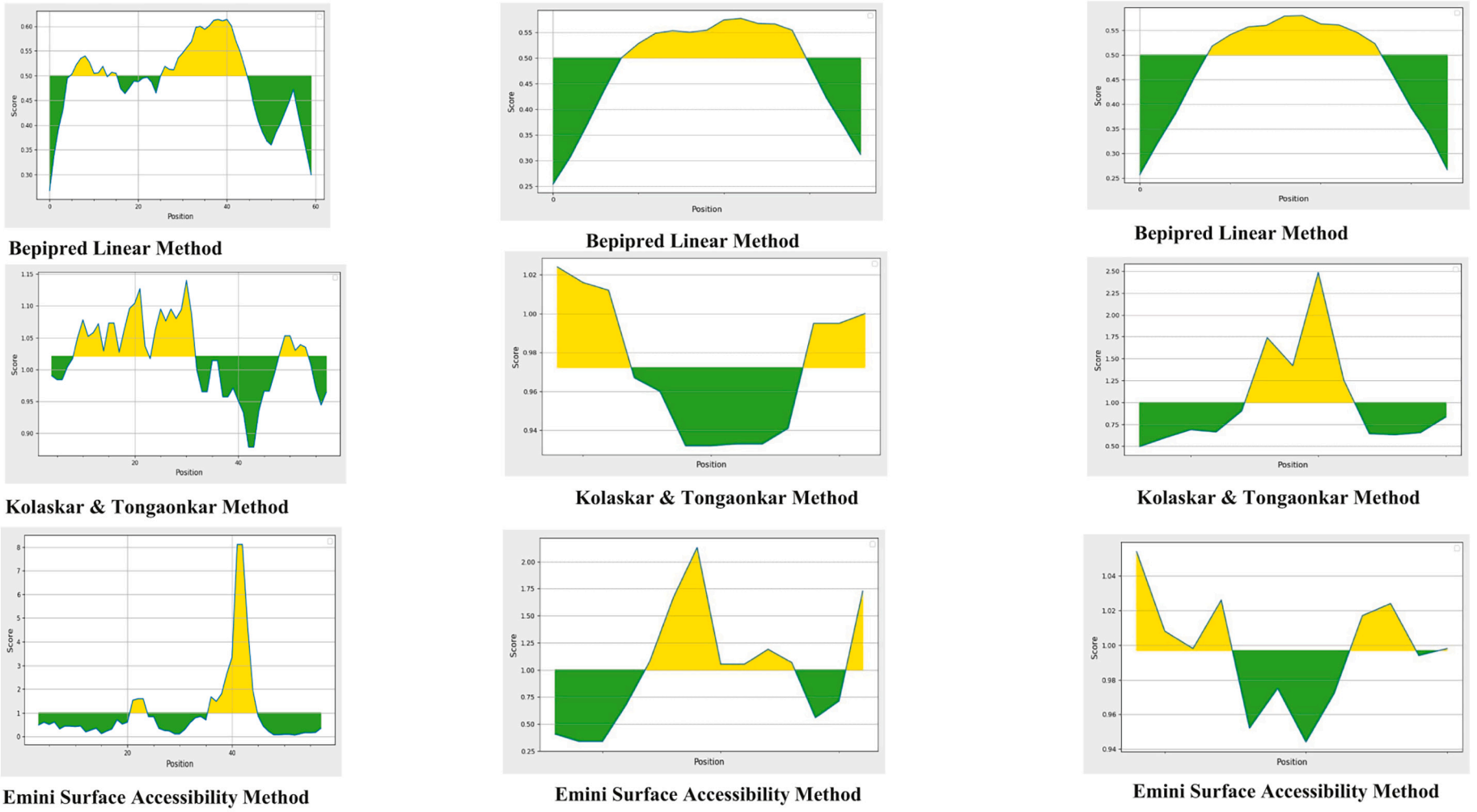

Fig. 3. Using different sizes, forecast B cell epitopes and intrinsic features for proteins (A) Hemagglutinin; (B) Neuraminidase; and (C) Matrix Protein 1 (1: Linear epitopes prediction, 2: Surface Accessibility, 3: Antigenicity). The X-axis depicts position, whereas the Y-axis depicts score. Residues that fall below the threshold value are shown in green, whereas favorable locations are shown in yellow. (For interpretation of the references to colour in this figure legend, the reader is referred to the web version of this article.)

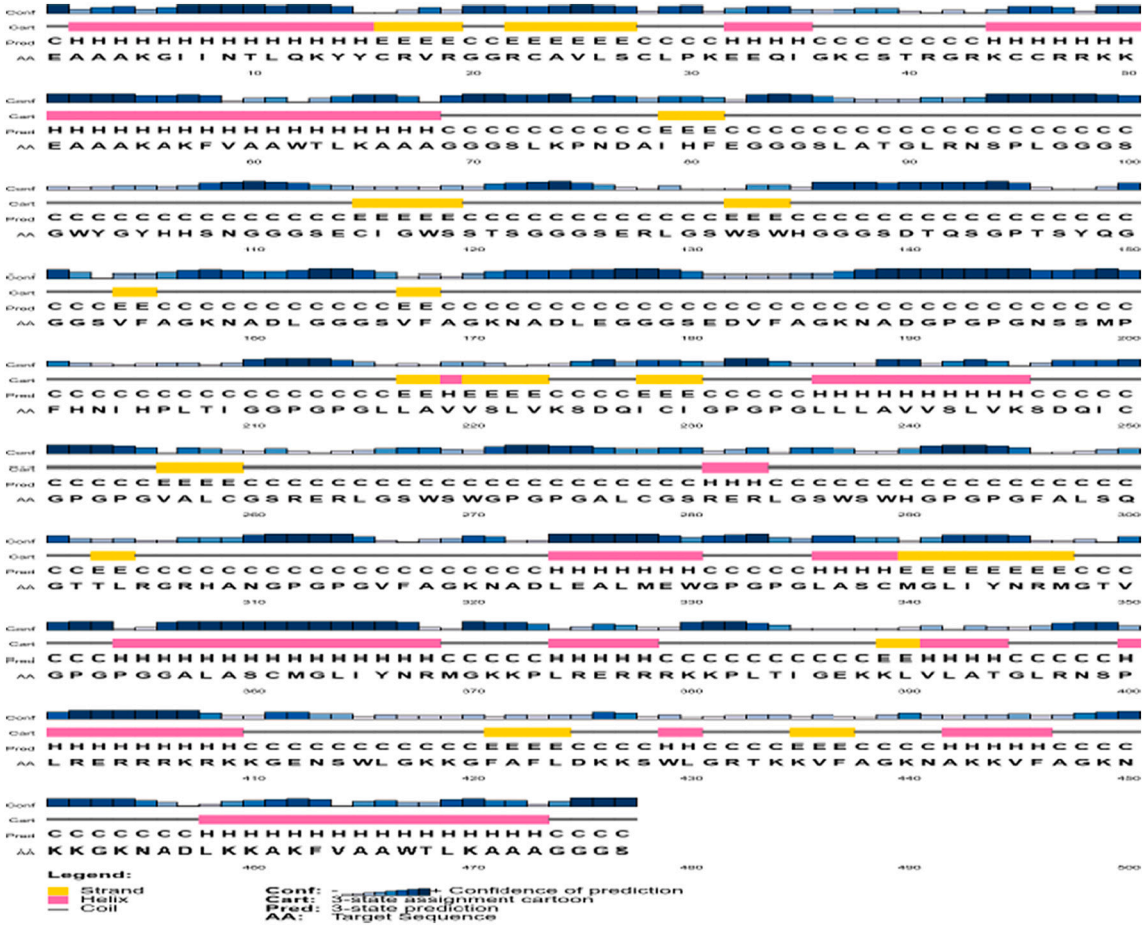

Fig. 4. Secondary structure prediction of designed vaccine V1 using PESIPRED server. Pink colour determine the helix structure and yellow colour determine the strand structure. (For interpretation of the references to colour in this figure legend, the reader is referred to the web version of this article.)

2.10. Molecular dynamics simulation and adaptation of codon cloning, and similarity analysis

The iMODS server's normal modes analysis (NMA) approach was utilized to deduce the overall motion of proteins (López-Blanco et al., 2014). The server predicted the trajectory and measure of complex dynamics using eigenvalue, covariance, deformability and B-factors (Awan et al., 2017) (Fig. 10).

The cloning and expression efficiency of the multi-epitope peptide-based vaccine construct is essential for vaccine design (Singh et al., 2020; Yousafi et al., 2021). Thus, in terms of codon adaptability, *E. coli* strain K12 was used as a cloning host for the vaccine design V1. Because human and *E. coli* codons are different, JCAT, a codon adaptation tool, was utilized to apply the codon to *E. coli* in order to boost expression. Rho-independent transcription termination, the binding site of the prokaryote ribosome, and *Bgl*II and Apa1 endonuclease restriction sites were all neglected during the process (Grote et al., 2005). The BglII restriction site was then ligated at the N-terminal of the transcribed sequence, while the Apa1 site was ligated at the C-terminal. SnapGene (Solanki and Tiwari, 2018), a restriction cloning tool, was used to load the adapted sequence between the BglII (401) and Apa (1334) positions in the pET28a(+) vector (Fig. 11).

3. Results

3.1. Retrieval of protein sequences and conserve regions analysis

The entire proteome of AIV H5N6 was extracted using the UniProtKB database (Proteome ID: UP000000826). Only the surface glycoprotein HA, NA and the multifunctional M1 were chosen for further study after examining the antigenic score, with overall prediction values of 0.5397, 0.5479, and 0.4531, respectively, due to their higher immunogenic potentials. The physiochemical properties of a number of proteins were then assessed, as shown in Table 1. Finally, conserved portions of selected proteins were investigated, and twelve conserved areas were chosen for their antigenic value (Supplementary Table1).

3.2. Anticipating of T-cell epitopes, and transmembrane topology and testing of epitope's allergenicity with toxicity

A large number of immunogenic epitopes were identified as potential T cell epitopes for any protein that can adhere to a significant percentage of HLA-A and HLA-B alleles using IEDB's MHC class I and II binding predictions. Epitopes with a high binding sensitivity and the ability to interact with a large variety of HLAs were chosen. The best epitopes for both proteins capable of eliciting a T-cell response were then picked as potential T cell epitope candidates using TMHMM's topological screening (Tables 2 and 3). The epitopes were shown to be non-toxic and non-allergenic in allergenicity and toxicity testing (Supplementary Tables 2, 3 and 4).

3.3. Measuring of population coverage and MHC restricted alleles conservancy analysis

The assessment resource 'The IEDB population covering computation tool' demonstrated population coverage at each unique epitope. The

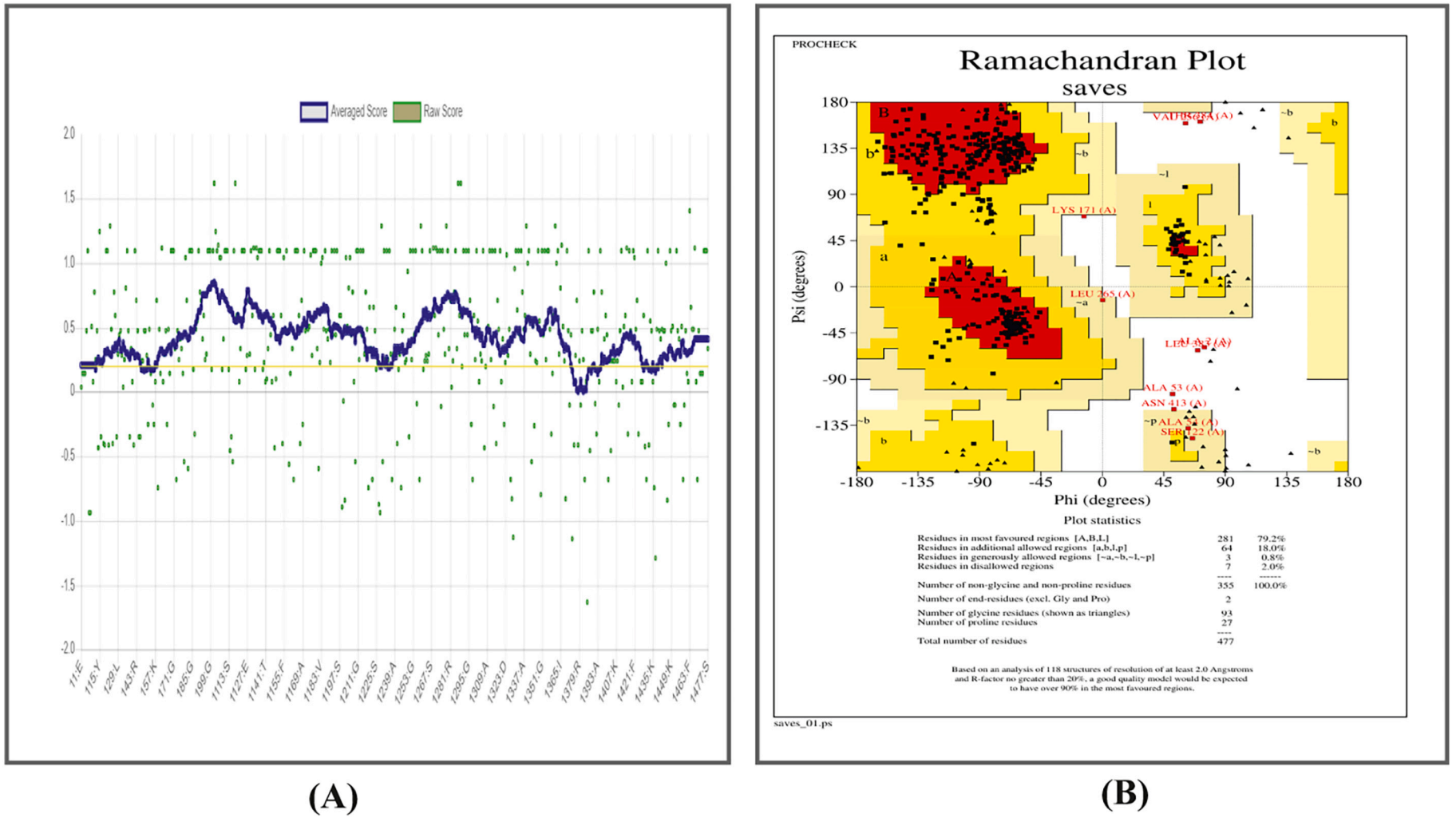

Fig. 5. Tertiary structure prediction and validation of vaccine protein V1, A: Verify3D shows a score of 91.82% % for our selected vaccine mode (blue colour determines the average score), B: Validation of the 3D structure of vaccine protein V1 by Ramachandran plot analysis depicting 79.2% of the residues to be in favorite regions score. (For interpretation of the references to colour in this figure legend, the reader is referred to the web version of this article.)

Table 1
ProtParam analysis of selected structural proteins.

Protein	Accession ID	Molecular Weight	Instability Index	Half-life	Theoretical pI	No. of Amino acids	Total No. of Atoms	Extinction Co-efficient	VaxiJen score
Hemagglutinin	A0A0K0YAR7	64,235.01	38.66	30 h	6.77	566	8940	93,125	0.5397 (ANTIGEN)
Neuraminidase	A0A0K0YAP8	50,747.53	44.03	30 h	6.56	459	7027	86,495	0.5479 (ANTIGEN)
Matrix Protein 1	A0A0K0YAP5	27,686.93	34.32	30 h	9.15	252	3897	13,075	0.4531 (ANTIGEN)

Table 2
Predicted T-cell epitopes (MHC-I peptides) of Hemagglutinin, Neuraminidase and Matrix protein 1 proteins.

Epitope	Start	End	Topology	No. of HLAs binding epitope	Antigenic score (AS)
Hemagglutinin					
LKPNDAIHFE	9	18	Outside	27	1.2660
LATGLRNSPL	29	38	Outside	27	1.0546
GWYGYHHSN	5	13	Outside	27	0.9621
Neuraminidase					
ECIGWSSTS	23	31	Outside	27	1.7616
ERLGSWSWH	12	20	Outside	27	1.5421
DTQSGPTSYQ	15	24	Outside	27	1.2992
Matrix Protein 1					
VFAGKNADL	4	12	Outside	27	1.4133
VFAGKNADLE	4	13	Outside	27	1.3896
EDVFAGKNAD	3	12	Outside	27	1.2556

Table 3
Predicted T-cell epitopes (MHC-II peptides) of Hemagglutinin, Neuraminidase and Matrix protein 1 proteins.

Epitope	Start	End	Topology	No. of HLAs binding epitope	AS
Hemagglutinin					
NSSMPFHNIHPLTIG	2	16	Outside	27	1.3970
LLAVVSLVKSDQICI	29	43	Outside	27	1.0816
LLLAVVSLVKSDQIC	28	42	Outside	27	0.9119
Neuraminidase					
ALCGSRERLGSWSWH	6	20	Outside	27	**1.1710**
VALCGSRERLGSWSW	5	19	Outside	27	**1.0221**
FALSQGTTLRGRHAN	1	15	Outside	27	**1.0104**
Matrix Protein 1					
VFAGKNADLEALMEW	4	18	Outside	27	0.8682
LASCMGLIYNRMGTV	4	18	Outside	27	0.6112
GALASCMGLIYNRMG	2	16	Outside	27	0.5234

demographic range of all of the alleles displayed in Fig. 2 was computed after they were shown to be effective binders with the specified epitopes. Two different inhabitant coverages were computed for MHC class I and II restricted peptides, employing CTL and HTL populations, respectively (Larsen et al., 2007). Several epitopes with higher vaxijen score from the surface glycoprotein HA, NA and the multifunctional M1 were found to be highly conserved among the dissimilar strain of AIV-A (H5N6), with the highest value of 100% conservation (Table 4). (See Table 5.)

3.4. Screening of B cell epitopes and construction of vaccine

The best peptide sequences that were shown to be extremely effective for greater antigenicity and non-allergenic features were enlisted in this phase (Table 6). The Bepipred linear prediction algorithm found peptide sequences capable of triggering immunological responses as B cell epitopes based on the literature. The Kolaskar and Tongaonkar Antigenicity algorithms (Fig. 3) were employed to find very antigenic epitopes, whereas the Emini Surface Accessibility prediction method was utilized to forecast more accessible epitopes. Then, each of the three

Table 4
Allergenicity assessment, toxicity test, and conservancy analysis of the predicted epitopes generated from Hemagglutinin, Neuraminidase and Matrix protein 1 proteins.

Epitope	Allergenicity	Toxicity	Conservancy (%)
Hemagglutinin			
LKPNDAIHFE	Non-Allergen	Non-Toxic	100.00%
LATGLRNSPL	Non-Allergen	Non-Toxic	100.00%
GWYGYHHSN	Non-Allergen	Non-Toxic	100.00%
NSSMPFHNIHPLTIG	Non-Allergen	Non-Toxic	100.00%
LLAVVSLVKSDQICI	Non-Allergen	Non-Toxic	100.00%
LLLAVVSLVKSDQIC	Non-Allergen	Non-Toxic	100.00%
Neuraminidase			
ECIGWSSTS	Non-Allergen	Non-Toxic	100.00%
ERLGSWSWH	Non-Allergen	Non-Toxic	100.00%
DTQSGPTSYQ	Non-Allergen	Non-Toxic	100.00%
VALCGSRERLGSWSW	Non-Allergen	Non-Toxic	100.00%
ALCGSRERLGSWSWH	Non-Allergen	Non-Toxic	100.00%
FALSQGTTLRGRHAN	Non-Allergen	Non-Toxic	100.00%
Matrix Protein 1			
VFAGKNADL	Non-Allergen	Non-Toxic	100.00%
VFAGKNADLE	Non-Allergen	Non-Toxic	100.00%
EDVFAGKNAD	Non-Allergen	Non-Toxic	100.00%
VFAGKNADLEALMEW	Non-Allergen	Non-Toxic	100.00%
LASCMGLIYNRMGTV	Non-Allergen	Non-Toxic	100.00%
GALASCMGLIYNRMG	Non-Allergen	Non-Toxic	100.00%

Table 5
Binding energy of suggested T cell epitopes with selected class I and class II MHC molecules generated from molecular docking analysis.

T-cell epitopes	Epitope	Patch Dock server	
		Score	Area
MHC-I	VFAGKNADL	8526	1032.50
	LATGLRNSPL	8362	1118.40
	ECIGWSSTS	8372	1096.20
	DTQSGPTSYQ	9040	1079.70
	EDVFAGKNAD	8700	1027.30
	VFAGKNADLE	8540	1029.90
	LKPNDAIHFE	9926	1170.00
	GWYGYHHSN	8252	1019.10
	ERLGSWSWH	9072	1158.90
MHC-II	GALASCMGLIYNRMG	11,252	1433.70
	VALCGSRERLGSWSW	11,090	1540.70
	VFAGKNADLEALMEW	11,122	1303.20
	ALCGSRERLGSWSWH	11,610	1454.40
	LASCMGLIYNRMGTV	11,082	1378.80
	NSSMPFHNIHPLTIG	12,396	1570.10
	LLAVVSLVKSDQICI	11,118	1221.70
	LLLAVVSLVKSDQIC	11,060	1391.80
	FALSQGTTLRGRHAN	11,134	11,134

Table 6
Allergenicity pattern of the predicted B-cell epitopes generated from envelope Hemagglutinin, Neuraminidase and Matrix protein 1 proteins.

Protein	Start	End	Peptide	Allergenicity
Hemagglutinin	37	43	PLRERRR	NON-ALLERGEN
	12	17	PLTIGE	NON-ALLERGEN
	27	45	LVLATGLRNSPLRERRRKR	NON-ALLERGEN
Neuraminidase	8	14	GENSWLG	NON-ALLERGEN
	2	7	GFAFLD	NON-ALLERGEN
	11	16	SWLGRT	NON-ALLERGEN
Matrix protein 1	4	10	VFAGKNA	NON-ALLERGEN
	4	9	VFAGKN	NON-ALLERGEN
	7	12	GKNADL	NON-ALLERGEN

vaccine designs was connected to a distinct protein adjuvant with a PADRE peptide sequence. B and T-cell epitopes, as well as their accompanying linkers, made up the leftover structures. In addition, the PADRE sequence was inserted to improve the vaccine protein's potency and efficiency. Each vaccine candidate has nine CTL, nine HTL, and nine BCL epitopes with GGGS, GPGPG and KK connections. There are 477, 562, and 591 residues in the vaccine candidates V1, V2, and V3, respectively (Table 7).

3.5. Antigenicity, allergenicity and solubility of the designed vaccine constructs and analysis of secondary structure, physicochemical properties with secondary and tertiary structure prediction

The vaccine designs (V1, V2, and V3) including beta-defensins 1 adjuvant, ribosomal protein adjuvant, and HABA adjuvant were declared non-allergic by both AlgPred and AllerTOP v.2.0. All of the vaccine designs were highly immunogenic. However, V1 outperformed the other structures in terms of solubility. The compound was non-allergic, highly soluble and antigenic, according to V2 (Table 7).

The ProtParam tool from the Expasy service was then used to characterize the physicochemical properties of the chosen vaccination candidate. The molecular weight of the produced vaccine construct V1 was 49.16 kDa, indicating that it had substantial immunogenic potential. The protein would have the above net negative charge if its theoretical pI was 10.16, and vice versa. If all cysteine residues were removed, the extinction coefficient was 82,680 at 0.1% absorption (Table 9). The half-life in mammalian reticulocytes in vitro was estimated to be 1 h, but it was estimated to be >10 h in *E. coli* in vivo. The protein's hydrophilic behavior and thermostability are demonstrated by the GRAVY value (−0.395) and aliphatic index (65.95). The protein's physicochemical characteristics indicated that it was stable and capable of eliciting a significant immune response from the body. Furthermore, the secondary structure of the chosen vaccine candidate was validated using the percent of alpha-helix (26.20%), strand (11.95%), and coil structure (61.85%) (Fig. 4). The tertiary structures of the vaccine candidate generated by raptor x were shown in Fig. 6.

3.6. Molecular modeling and docking

Docking against several HLA alleles resulted in successful valid modeling and model consistency evaluation. V1 was superior in terms of binding energy (Table 8); hence, V1 is regarded as the strongest, having docked with TLR 8 (PDB: 3W3M) and binds efficiently (Fig. 8). TLR8 agonists' ability to activate dendritic cells and thus elicit Th1 and CD8+ T cell responses can be used to improve peptide based vaccine efficacy (Rahman et al., 2020). Figs. 5 and 7 illustrate the anticipated model and vaccine construct accuracy, respectively, as created by proSa-web server (Wiederstein and Sippl, 2007).

3.7. Molecular dynamics simulation

Protein stability and motility can be explained using regular mode analysis. The internal coordinates of the protein-protein complex are used by the iMODS server for this study. The movement's direction is indicated by the arrows in Fig. 10A, and the length of the line indicates the movement's range. According to the observations, V1 and TLR 8 are focused on each other. The presence of chain hinges suggests that the docked complex may be deformable. The NMA provided the B-factor values, which are equivalent to RMS (Fig. 10C). The eigenvalue of the complex was 7.086112e-06 (Fig. 10B). The bigger the eigenvalue, the less the variance associated with each NMA investigation, and vice

Table 7
Allergenicity and antigenicity analysis of the constructed vaccines.

Composition	Complete Sequence of Vaccine Constructs	Allergenicity	Solubility	VaxiJen score
V1	EAAAKGIINTLQKYYCRVRGGRCAVLSCLPKEEQIGKCSTRGRKCCRRKKEAAAKAKFVAAWTL KAAAGGGSLKPNDAIHFEGGGSLATGLRNSPLGGGSGWYGYHHSNGGGSECIGWSSTSGG GSERLGSWSWHGGGSDTQSGPTSYQGGGSVFAGKNADLGGGSVFAGKNADLEGGGSEDVFAGKNADGP GPGNSSMPFHNIHPLTIGGPGPGLLAVVSLVKSDQICIGPGPGLLLAVVSLVKSDQICGPGPGVALCGSRERLG SWSWGPGPGALCGSRERLGSWSWHGPGPGFALSQGTTLRGRHANGPGPGVFAGKNADLEALMEWGPGP GLASCMGLIYNRMGTVGPGPGGALASCMGLIYNRMGKKPLRERRRKKPLTIGEKKLVLATGLRN SPLRERRRKRKKGENSWLGKKGFAFLDKKSWLGRTKKVFAGKNAKKVFAGKNKKGKNAD LKKAKFVAAWTLKAAAGGGS	NON-ALLERGEN	0.663	0.6474
V2	EAAAKMAKLSTDELLDAFKEMTLLELSDFVKKFEET FEVTAAAPVAVAAAGAAPAGAAVEAAEEQSEFDVILEAAGDKKIGVIKVVREIVSGL GLKEAKDLVDGAPKPLLEKVAKEAADEAKAKLEAAGATVTVKEAAAKAKFV AAWTLKAAAGGGSLKPNDAIHFEGGGSLATGLRNSPLGGGSGWYGYHHSNGGGSECIGWSSTSGGGSERL GSWSWHGGGSDTQSGPTSYQGGGSVFAGKNADLGGGSVFAGKNADLEGGGSEDVFAGKNADGPGPGN SSMPFHNIHPLTIGGPGPGLLAVVSLVKSDQICIGPGPGLLLAVVSLVKSDQICGPGPGVALCGSRERLGSWSW GPGPGALCGSRERLGSWSWHGPGPGFALSQGTTLRGRHANGPGPGVFAGKNADLEALMEWGPGPGLAS CMGLIYNRMGTVGPGPGGALASCMGLIYNRMGKKPLRERRRKKPLTIGEKKLVLATGLRNSPLRERRRKRKKG ENSWLGKKGFAFLDKKSWLGRTKKVFAGKNAKKVFAGKNKKGKNADLKKAKFVAAWTLKAAAGGGS	NON-ALLERGEN	0.609	0.5983
V3	EAAAKMAENPNIDDLPAPLLAALGAADLALATVNDLI ANLRERAEETRAETRTRVEERRARLTKFQEDLPEQFIELRDKFTTEELRKAAEGYLEAATNRYNELVERGE AALQRLRSQTAFEDASARAEGYVDQAVELTQEALGTVASQTRAVGERAAKLVGIELEAAAKAKFVAAWTLK AAAGGGSLKPNDAIHFEGGGSLATGLRNSPLGGGSGWYGYHHSNGGGSECIGWSSTSGGGSERLGSWSWH GGGSDTQSGPTSYQGGGSVFAGKNADLGGGSVFAGKNADLEGGGSEDVFAGKNADGPGPGNSSMPFHNI HPLTIGGPGPGLLAVVSLVKSDQICIGPGPGLLLAVVSLVKSDQICGPGPGVALCGSRERLGSWSWGPGPGAL CGSRERLGSWSWHGPGPGFALSQGTTLRGRHANGPGPGVFAGKNADLEALMEWGPGPGLASCMGLIYNR MGTVGPGPGGALASCMGLIYNRMGKKPLRERRRKKPLTIGEKKLVLATGLRNSPLRERRRKRKKGENSWLG KKGFAFLDKKSWLGRTKKVFAGKNAKKVFAGKNKKGKNADLKKAKFVAAWTLKAAAGGGS	NON-ALLERGEN	0.594	0.6162

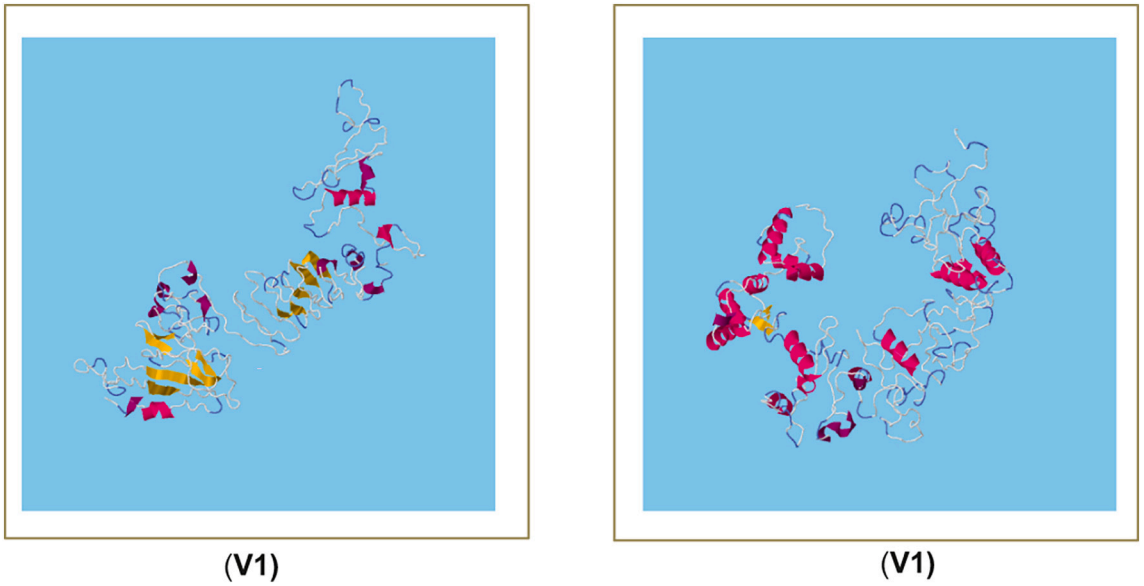

Fig. 6. 3D modeled structure of vaccine protein V1 and V2 generated via Raptor-X server.

versa. The coupling of residues was visualized using a covariance matrix, with red, blue and white colors denoting clustered, anti-correlated, and uncorrelated motions, respectively (Fig. 10E). An elastic network model (Fig. 10F) and variance are used to investigate the pairs of atoms connected by springs (Fig. 10D).

3.8. Disulfide bonds simulation of the selected vaccine candidate and adaptation of codon cloning, and similarity analysis

Using the DbD2 server, a total of 63 amino acid pairings with the capacity to form disulfide bonds were discovered. Only three sequences (LEU 29-GLY 85, ALA 173-GLY 179, and ALA 276-ALA 297) were discovered to be convenient for disulfide bond formation after considering the energy, chi3, and B-factor criteria. A chi3 value of 87 to +97 and an energy of 2.5 were used in residue screening. Then, to create a mutant model, all of these residues were substituted with cysteine residues (Fig.9). Then, the Codon Adaptation Index (CAI) was 1.0, indicating that the most common codons were employed in the most cases. The GC content was satisfactory (53.249%) after correction, and the series lacked the *Bgl*II and *Apa*I restriction sites, making cloning more appealing. The adopted sequence was then inserted between the BglII and ApaI restriction sites in the pET28a(+) vector. The final clone was 5877 bp long, with a 1441 bp embedded segment and the remainder being vector (Fig. 11). The red hue is used to draw attention to the extracted area.

4. Discussion

Multiple viral epidemics have emerged in recent years, posing an invisible threat to both human and animal populations. Furthermore, reassortment between different subtypes of the same virus not only aggravates the situation but also emerges a new subtype, of which AIV-A (H5N6) is one. Thus, to deter the severity of deadly AIV-A (H5N6), vaccination is considered as the most fundamental and safest way. Recent advances in immunoinformatics, bioinformatics and structural vaccinomics have revolutionized antigen screening and aided a novel vaccine development strategy to construct vaccines against a wide range of bacterial and viral infections (Capelli et al., 2018; Soltan et al., 2021). In previous studies, the multi epitope peptide vaccine has been shown to have greater efficacy and protection against infectious agents than single epitope-based vaccines (Bourdette et al., 2005; Knutson et al., 2001; Lpez et al., 2001). Keeping this sense, the current study focused on subunit vaccines, which are constructed with numerous immunogenic components of pathogens and have the ability to focus the humoral immune response on specific antigenic epitopes, resulting in a more safe

Table 8
Binding energy of predicted epitopes with selected MHC class I and II molecules generated from molecular docking.

Vaccine Construct	HLA alleles PDB ID's	ClusPro 2.0 server	
		Energy score	
V1	1A6A	Center	−890.8
		Lowest	−1168.6
	1H15	Center	−967.8
		Lowest	−1257.3
	2SEB	Center	−999.2
		Lowest	−1144.8
	2Q6W	Center	−940.5
		Lowest	−1075.1
	2FSE	Center	−980.8
		Lowest	−1252.3
	3C5J	Center	−1111.4
		Lowest	−1184.7
V2	1A6A	Center	−866.4
		Lowest	−982.3
	1H15	Center	−950.6
		Lowest	−1043.1
	2SEB	Center	−994.5
		Lowest	−994.5
	2Q6W	Center	−854.1
		Lowest	−1117.0
	2FSE	Center	−977.5
		Lowest	−1052.0
	3C5J	Center	−984.0
		Lowest	−991.7
V3	1A6A	Center	−1281.9
		Lowest	−1473.2
	1H15	Center	−1076.6
		Lowest	−1076.6
	2SEB	Center	−1140.7
		Lowest	−1575.4
	2Q6W	Center	−953.4
		Lowest	−1421.1
	2FSE	Center	−1018.8
		Lowest	−1131.2
	3C5J	Center	−1131.5
		Lowest	−1303.7
V1	3W3M (TLR 8)	Center	−891.3
		Lowest	−1033.1

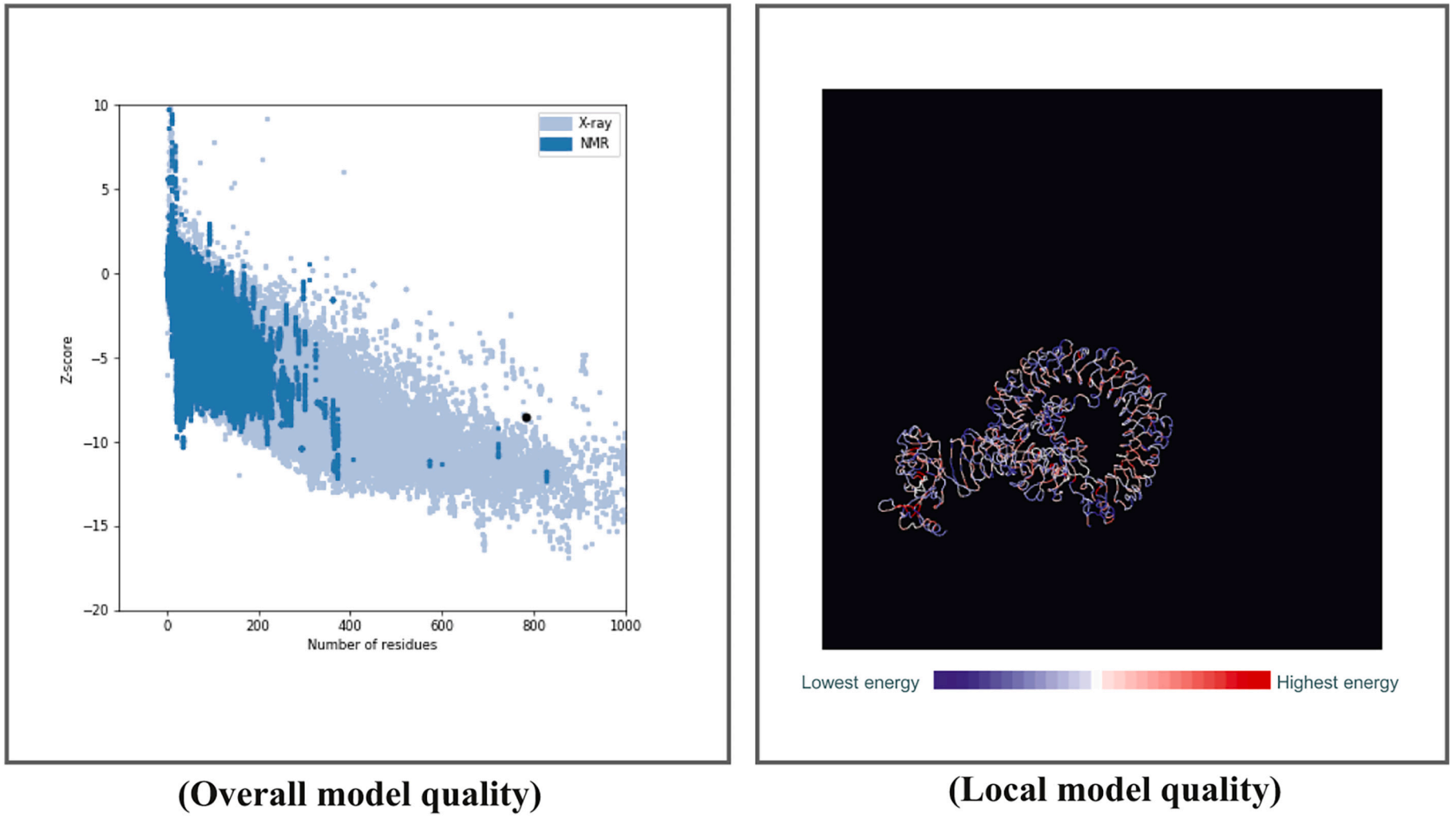

Fig. 7. Vaccine 1-TLR 8 complex validations using ProSAweb tool, revealing a *Z*-score of −8.55. The Z-Score plot shows the z-scores of all investigational protein chains in the PDB that were determined by NMR spectroscopy (dark blue) and X-ray crystallography (light blue). (For interpretation of the references to colour in this figure legend, the reader is referred to the web version of this article.)

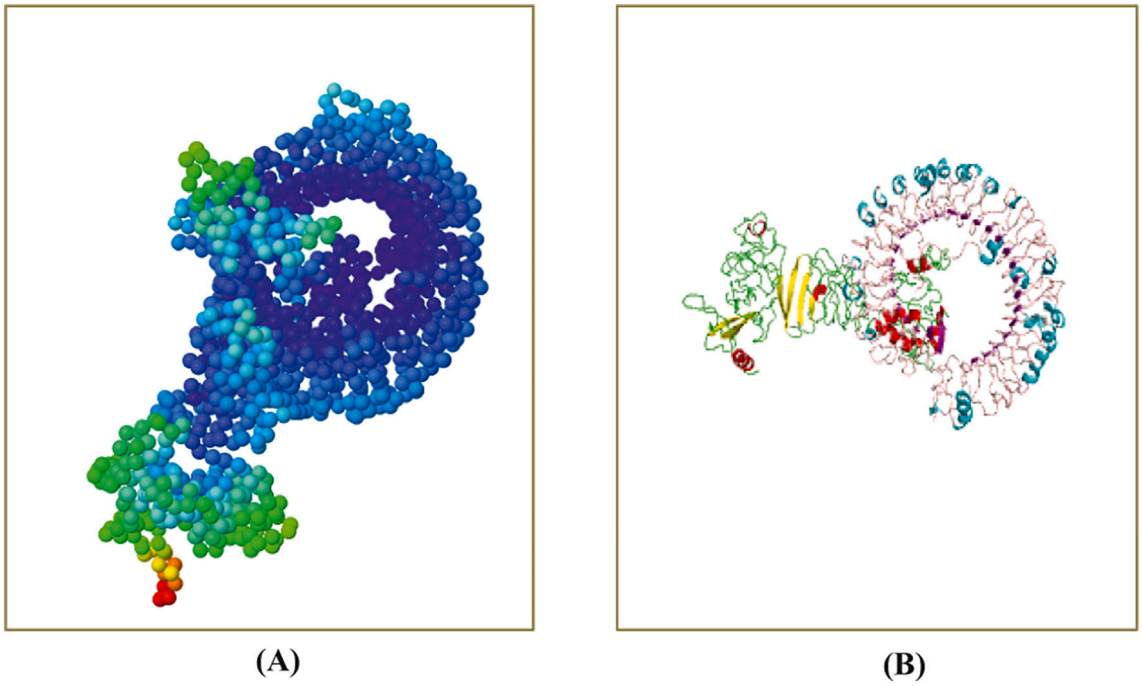

Fig. 8. Docked complex of vaccine construct V1 with human TLR8; A: Spacefill format and B: structure by ClusPro server represents the formation of stable complex.

and effective immune response (ul Qamar et al., 2020).

In the present study, we used the NCBI database to retrieve viral three outer proteins of AIV-A (H5N6) strains after a thorough literature analysis. The ProtParam server was used to analyze the physiochemical characteristics of viral proteins. (Das et al., 2015). Moreover, the VaxiJen server assessed all of the retrieved protein sequences in order to find out the most potent antigenic protein and ability to confer immunity. Two viral proteins including, HA (Accession ID: A0A0K0YAR7) and NA (Accession ID: A0A0K0YAP8) are the surface glycoprotein responsible for binding to host cell (Russell et al., 2008) while another protein named as matrix M1 (Accession ID: A0A0K0YAP5) (inner membrane protein) is one of the most abundant proteins of influenza A virus playing essential structural and functional roles in the virus life cycle (Shtykova et al., 2013). Besides, previous studies confirmed good antibody response in the host induced via M1 (Lohia and Baranwal, 2017).

Vaccines cause B cells to produce antibodies, which then mediate effector actions by engaging specifically with a pathogen or toxin. Given their involvement in retaining memory cells, longer life and guarding against reinfection, the humoral immune response has a clear role in vaccine-mediated protection against infections. Most antigens and vaccinations elicit a T cell response in addition to a B cell response (Amanna and Slifka, 2011; Shtykova et al., 2013). Another important immune cell type that obtains Th1 or Th2 phenotypes and drives immunological responses is the CD4+ T cell (HTL/MHC-II) (Khan et al., 2021). Th1 response activates cytotoxic CD8 + T lymphocytes (CTL/MHC-I) natural killer cells, and macrophages, whereas Th2 is responsible for B cell

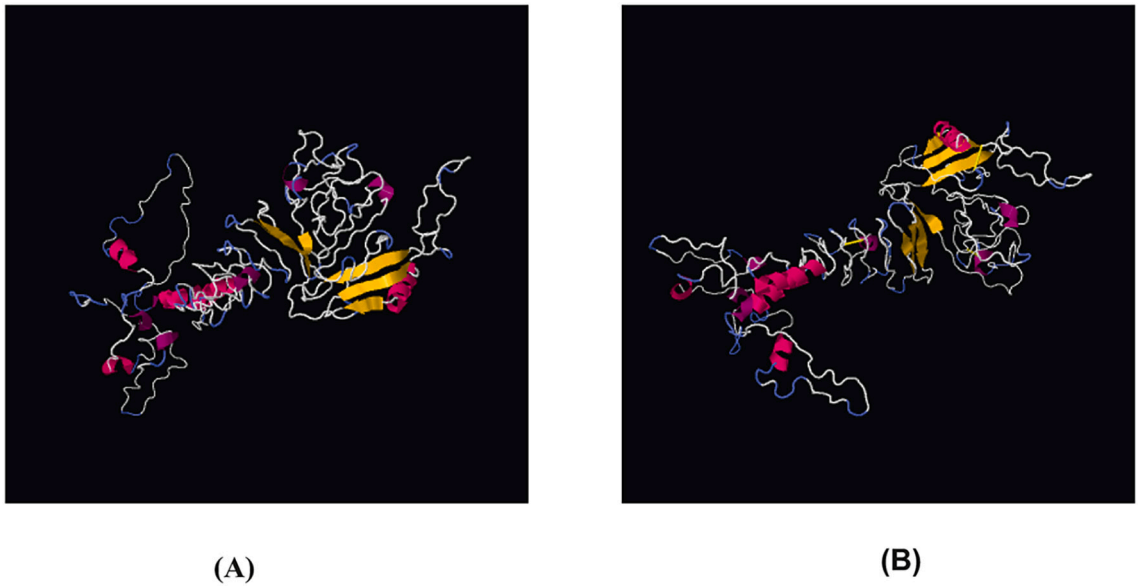

Fig. 9. Disulfide engineering of vaccine protein V1; A: Initial form, B: Mutant form. Yellow colour determines the hydrogen bonds. (For interpretation of the references to colour in this figure legend, the reader is referred to the web version of this article.)

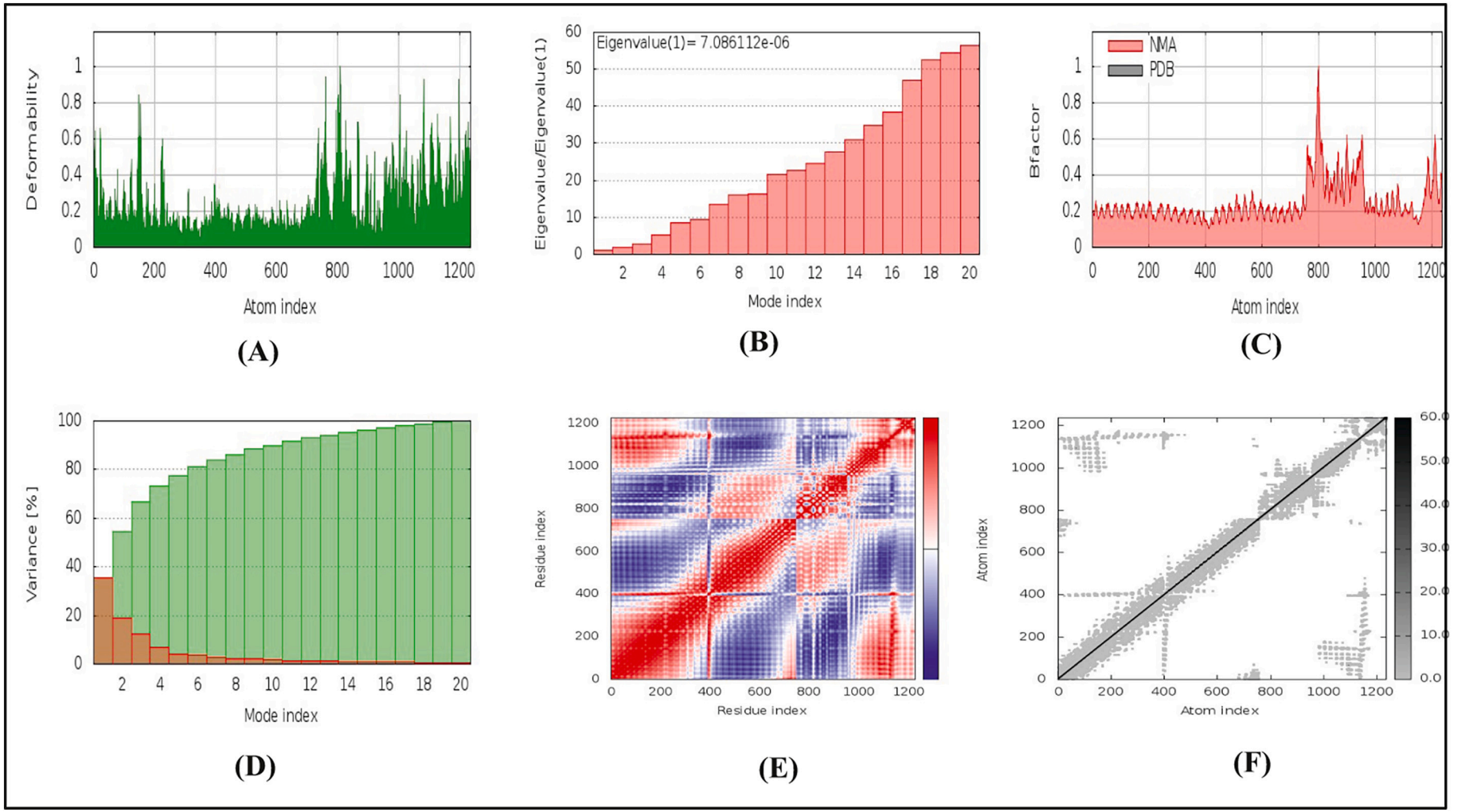

Fig. 10. Molecular dynamics simulation of vaccine protein V1-TLR8 complex. Stability of the protein-protein complex was investigated through deformability (A), eigenvalue (B), B-factor (C), variance (D), covariance indicates coupling between pairs of residues (red), uncorrelated (white) or anti-correlated (blue) motions (E) and elastic network analysis which defines which pairs of atoms are connected by springs (F). (For interpretation of the references to colour in this figure legend, the reader is referred to the web version of this article.)

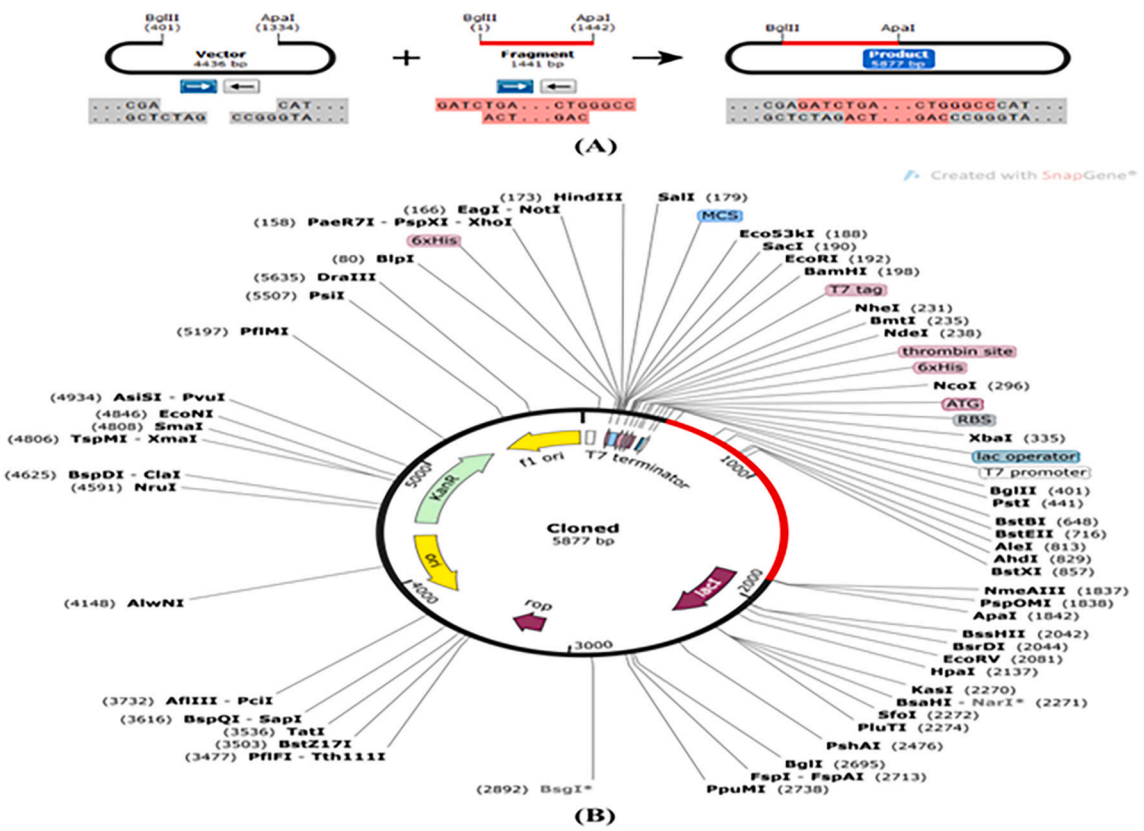

Fig. 11. In silico restriction cloning of the gene sequence of selected designed vaccine V1 into pET28a(+) expression vector; (A) Restriction digestion of the vector pET28a(+) and construct V1 with *Bgl*II and *Apa*I (B) Inserted desired fragment (V1 Construct) between BglII (401) and ApaI (1334) indicated in red colour. Inserted fragment marked in red colour. (For interpretation of the references to colour in this figure legend, the reader is referred to the web version of this article.)

activation, isotype switching, affinity maturation, and antibody generation that kills external pathogens (Lafuente and Reche, 2009). Thus, T cell epitope-based vaccination is a unique process to induce strong immune response against infectious agents (Shrestha and Diamond, 2004). In this study, we used the IEDB's MHC-I and MHC-II binding predictions, as well as topology screening and the VaxiJen score, to screen for potential CTL (MHC-I) and HTL (MHC-II) immunogenic epitopes of hemagglutinin, neuraminidase, and matrix protein 1 that can bind a large number of HLA-A and HLA-B alleles with high binding affinity. AllerTOP, Allergen FP, Allermatch, and Allergen Online were used in this work to examine the allergenicity of T-cell epitopes of proteins. In the immune stimulation process, allergenicity, a major barrier in vaccine development, was discovered in most vaccine candidates as an "allergic" reaction. The World Health Organization has an allergenicity prediction method that states that a sequence could be potentially allergenic if it has an identity of at least six contiguous amino acids over an 80 amino acid window when compared to known allergens (McKeever et al., 2011). Aside from that, population coverage is a potential parameter in the reverse vaccinology technique. All anticipated T cell epitopes of HA, NA, and M1 can cover populations from most geographic parts of the world, according to the findings (>90%). MHC cluster analysis was also undertaken to establish the functional link between MHC variations, as MHC superfamilies play an important role in vaccine design and medication development.

For identifying probable B-cell epitopes, we employed four algorithms from the IEDB server's Linear B-cell epitope prediction method to predict amino acid scale-based methodologies. Though numerous B-cell epitope prediction approaches have been developed without very much success over the last few decades, experimental epitope determination has mostly focused on the identification of a linear B-cell epitope prediction method (El-Manzalawy and Honavar, 2010). Moreover, linear B-cell epitope prediction can aid in accurate prediction as well as a speedier and less expensive vaccine design procedure. (Galanis et al., 2021). Thus, the most potent B cell epitopes for the three proteins were selected as vaccine candidates AIV-A (H5N6) strain using Kolaskar and Tongaonkar antigenicity scale, Emini surface accessibility prediction, and Bepipred linear epitope prediction 2.0. Promiscuous epitopes and protein adjuvants, as well as the PADRE peptide sequence, were used to create the final vaccine proteins. Adjuvants were previously used as immunomodulator to enhance the activity of several vaccine candidates (Mohan et al., 2013; Solanki and Tiwari, 2018). Beta defensin adjuvant has already been proved as an effective immune-stimulator against different organisms in a number of experiments (Mohan et al., 2013).

In this study, three vaccinations were created using an approach in which each epitope was bonded separately using appropriate linkers. PADRE-containing vaccine designs also demonstrated greater CTL responses than vaccinations without it, according to studies (Wu et al., 2010). The vaccines were also tested for their non-allergic properties

Table 9
Physicochemical properties of vaccine construct (V1).

Physical properties	
Number of amino acids	477
Molecular weight	49,162.30
Theoretical pI	10.16
Formula	$C_{2160}H_{3446}N_{658}O_{620}S_{19}$
Total number of atoms	6903
Extinction coefficients	82,680
Estimated half-life	>10 h (*Escherichia coli*, in vivo)
Instability index	33.59
Aliphatic index	65.95
Grand average of hydropathicity (GRAVY)	−0.395

and immunogenic potential. In terms of antigenicity, solubility and allergenicity, Construct V1 was determined to be superior. Before predicting tertiary structure and refining the 3D model, the physicochemical characteristics and secondary structure of V1 were investigated. The produced vaccine construct V1 has a molecular weight of 49.16 kDa, which is higher than the previously reported AIV vaccine candidate (Behbahani et al., 2021), and it is revealed that an acceptable vaccine because proteins with a molecular weight of <110 kDa are considered to be more appropriate targets for vaccine development due to rapid purification (Barh et al., 2013). Furthermore, the aliphatic index and GRAVY value of the predicted vaccine candidate was 65.95 and (−0.395), which were slightly higher than the previous AIV vaccine candidate's aliphatic index (Behbahani et al., 2021) and GRAVY value (Shahsavandi et al., 2015). The higher the aliphatic index value, the greater the thermostability, and higher negative the GRAVY value, the more hydrophilic the vaccine, and thus capable of interacting strongly with water molecules (Ali et al., 2017). Moreover, the secondary structure of the chosen vaccine candidate had a higher coil structure than previously proposed vaccine candidates against AIV, and it is concluded that random coils play an important role in the high flexibility of proteins and may enhance antibody binding ability (Shahsavandi et al., 2015).

To reinforce our prediction, we tested the interaction of our vaccine design with several HLA molecules (iDRB1*0101, DRB3*0202, DRB5*0101, DRB3*0101, DRB1*0401, and DRB1*0301). In terms of free binding energy, build V1 was shown to be the best. Furthermore, docking analysis was utilized to investigate the binding affinity of vaccine protein V1 and the human TLR8 receptor in order to assess the efficiency of the adjuvant used. Binding affinity is improved when the binding energy is low. After that, molecular dynamics simulation was used to determine the stability of the interactions. The interactions were found to be both flexible and stable, according to the research. After that, in silico cloning was done. In silico cloning was successful, indicating that the vaccine may be produced in huge quantities in *E. coli*. (Akhtar et al., 2021).

However, the computational vaccinology approach has some challenges, such as inability to conduct in vivo and intro test, rapid changing the software version, the inability to retrieve glycan-based epitopes using the protein-based reverse vaccinology process. Therefore, our projected in silico results were generated utilizing several immunological databases and diverse computational analysis of sequences. For experimental validation of the anticipated vaccine candidates, we recommend more wet lab-based research involving model animals.

5. Conclusion

Along with the continuing pandemic, the widespread transmission of the highly pathogenic AIV-A (H5N6) has raised new concerns. The situation is deteriorating as a consequence of migration-related dispersion. Thus, it will be difficult to implement control measures without an effective medicine or vaccine. In this regard, current study described a computational approach for multi-epitope-based peptide subunit vaccine prediction against AIV-A (H5N6). Based on a literature review, an immunoinformatics and structural vaccinology approach was used to build a multi epitope vaccine, which was confirmed using online tools to be an effective vaccination candidate against AIV-A (H5N6). To validate our findings, we suggest going the designed vaccine to the biological validation phase via animal model.

Funding

This research did not receive any specific grant from funding agencies in the public, commercial, or not-for-profit sectors.

Declaration of Competing Interest

The authors declare that they have no known competing financial interests or personal relationships that could have appeared to influence the work reported in this paper.

Authors declare that they have no conflict of interests.

Acknowledgements

The authors would like to acknowledge the Faculty of Veterinary, Animal and Biomedical Sciences, Sylhet Agricultural University for the technical support of the project.

Appendix A. Supplementary data

Supplementary data to this article can be found online at https://doi.org/10.1016/j.meegid.2022.105355.

References

Abu-Haraz, A.H., Abd-elrahman, K.A., Ibrahim, M.S., Hussien, W.H., Mohammed, M.S., Badawi, M.M., Salih, M.A., 2017. Multi epitope peptide vaccine prediction against Sudan Ebola virus using immuno-informatics approaches. Adv. Tech. Biol. Med. 5, 1764–2379. https://doi.org/10.4172/2379-1764.1000203.

Akhtar, N., Joshi, A., Kaushik, V., Kumar, M., Mannan, M.A., 2021. In-silico design of a multivalent epitope-based vaccine against Candida auris. Microb. Pathog. 155, 104879 https://doi.org/10.1016/j.micpath.2021.104879.

Ali, M., Pandey, R.K., Khatoon, N., Narula, A., Mishra, A., Prajapati, V.K., 2017. Exploring dengue genome to construct a multi-epitope based subunit vaccine by utilizing immunoinformatics approach to battle against dengue infection. Sci. Rep. 7, 1–13. https://doi.org/10.1371/journal.pone.0196484.

Alizadeh, M., Amini-Khoei, H., Tahmasebian, S., Ghatrehsamani, M., Ghatreh Samani, K., Edalatpanah, Y., Rostampur, S., Salehi, M., Ghasemi-Dehnoo, M., Azadegan-Dehkordi, F., others, 2022. Designing a novel multi-epitope vaccine against Ebola virus using reverse vaccinology approach. Sci. Rep. 12, 1–15. https://doi.org/10.1038/s41598-022-11851-z.

Almofti, Y.A., Abd-elrahman, K.A., Gassmallah, S.A.E., Salih, M.A., others, 2018. Multi epitopes vaccine prediction against severe acute respiratory syndrome (SARS) coronavirus using immunoinformatics approaches. Am. J. Microbiol. Res. 6, 94–114. https://doi.org/10.12691/ajmr-6-3-5.

Amanna, I.J., Slifka, M.K., 2011. Contributions of humoral and cellular immunity to vaccine-induced protection in humans. Virology 411, 206–215.

Awan, F.M., Obaid, A., Ikram, A., Janjua, H.A., 2017. Mutation-structure-function relationship based integrated strategy reveals the potential impact of deleterious missense mutations in autophagy related proteins on hepatocellular carcinoma (HCC): a comprehensive informatics approach. Int. J. Mol. Sci. 18, 139. https://doi.org/10.3390/ijms18010139.

Barh, D., Barve, N., Gupta, K., Chandra, S., Jain, N., Tiwari, S., Leon-Sicairos, N., Canizalez-Roman, A., dos Santos, A., Hassan, S.S., others, 2013. Exoproteome and secretome derived broad spectrum novel drug and vaccine candidates in vibrio cholerae targeted by Piper betel derived compounds. PLoS One 8, e52773.

Basak, S., Tomana, M., Compans, R.W., 1985. Sialic acid is incorporated into influenza hemagglutinin glycoproteins in the absence of viral neuraminidase. Virus Res. 2, 61–68.

Behbahani, M., Moradi, Mohammad, Mohabatkar, Hassan, 2021. In silico design of a multi-epitope peptide construct as a potential vaccine candidate for Influenza A based on neuraminidase protein. Silico Pharmacol. 91 (9), 1–13. https://doi.org/10.1007/S40203-021-00095-W.

Bi, Y., Chen, Q., Wang, Q., Chen, J., Jin, T., Wong, G., Quan, C., Liu, J., Wu, J., Yin, R., others, 2016. Genesis, evolution and prevalence of H5N6 avian influenza viruses in China. Cell Host Microbe 20, 810–821. https://doi.org/10.1016/j.chom.2016.10.022.

Bi, Y., Tan, S., Yang, Y., Wong, G., Zhao, M., Zhang, Q., Wang, Q., Zhao, X., Li, L., Yuan, J., others, 2019. Clinical and immunological characteristics of human infections with H5N6 avian influenza virus. Clin. Infect. Dis. 68, 1100–1109. https://doi.org/10.1093/cid/ciy681.

Bourdette, D.N., Edmonds, E., Smith, C., Bowen, J.D., Guttmann, C.R.G., Nagy, Z.P., Simon, J., Whitham, R., Lovera, J., Yadav, V., Mass, M., Spencer, L., Culbertson, N., Bartholomew, R.M., Theofan, G., Milano, J., Offner, H., Vandenbark, A.A., 2005. A highly immunogenic trivalent T cell receptor peptide vaccine for multiple sclerosis. Mult. Scler. 11, 552–561. https://doi.org/10.1191/1352458505MS1225OA.

Bui, H.-H., Sidney, J., Dinh, K., Southwood, S., Newman, M.J., Sette, A., 2006. Predicting population coverage of T-cell epitope-based diagnostics and vaccines. BMC Bioinform. 7, 1–5.

Capelli, R., Peri, C., Villa, R., Nithichanon, A., Conchillo-Solé, O., Yero, D., Gagni, P., Chiari, M., Lertmemongkolchai, G., Cretich, M., others, 2018. BPSL1626: reverse and structural vaccinology reveal a novel candidate for vaccine design against Burkholderia pseudomallei. Antibodies 7, 26.

CDC, C. for D.C. and P, 2021. CDC Update on A(H5N6) Bird Flu: How is the U.S. CDC Monitoring A(H5N6) Infections and Contributing to Global Pandemic Preparedness? CDC [WWW Document].
Cenmidtal, C., Rosari, S., 2011. Prediction of a neutralizing epitope of a H5N1 virus hemagglutinin complexed with an antibody variable fragment using molecular dynamics simulation. J. Biophys. Chem. 2011, 258–267. https://doi.org/10.4236/JBPC.2011.23031.
Criado, M.F., e Silva, M., Lee, D.H., Salge, C.A.D.L., Spackman, E., Donis, R., Wan, X.-F., Swayne, D.E., 2020. Cross-protection by inactivated H5 Prepandemic vaccine seed strains against diverse goose/Guangdong lineage H5N1 highly pathogenic avian influenza viruses. J. Virol. 94, e00720. https://doi.org/10.1128/JVI.00720-20.
Das, K., Chakraborty, S., Hasan, M., Maruf, A., Shovo, R., 2015. In silico analysis to elect superior bacterial alkaline protease for detergent and leather industries. J. Adv. Biotechnol. 5, 685–698. https://doi.org/10.24297/JBT.V5I3.1482.
De Jong, M.D., Simmons, C.P., Thanh, T.T., Hien, V.M., Smith, G.J.D., Chau, T.N.B., Hoang, D.M., Chau, N.V.V., Khanh, T.H., Dong, V.C., Qui, P.T., Van Cam, B., Ha, D. Q., Guan, Y., Peiris, J.S.M., Chinh, N.T., Hien, T.T., Farrar, J., 2006. Fatal outcome of human influenza a (H5N1) is associated with high viral load and hypercytokinemia. Nat. Med. 1210 (12), 1203–1207. https://doi.org/10.1038/nm1477.
Dimitrov, I., Bangov, I., Flower, D.R., Doytchinova, I., 2014a. AllerTOP v. 2—a server for in silico prediction of allergens. J. Mol. Model. 20, 1–6. https://doi.org/10.1007/s00894-014-2278-5.
Dimitrov, I., Naneva, L., Doytchinova, I., Bangov, I., 2014b. AllergenFP: allergenicity prediction by descriptor fingerprints. Bioinformatics 30, 846–851. https://doi.org/10.1093/bioinformatics/btt619.
Doytchinova, I.A., Flower, D.R., 2007. VaxiJen: a server for prediction of protective antigens, tumour antigens and subunit vaccines. BMC Bioinform. 8, 1–7. https://doi.org/10.1186/1471-2105-8-4.
El-Manzalawy, Y., Honavar, V., 2010. Recent advances in B-cell epitope prediction methods. Immun. Res. 6, 1–9.
Emini, E.A., Hughes, J.V., Perlow, D.S., Boger, J., 1985. Induction of hepatitis a virus-neutralizing antibody by a virus-specific synthetic peptide. J. Virol. 55, 836–839. https://doi.org/10.1128/JVI.55.3.836-839.1985.
Farooqui, A., Liu, W., Zeng, T., Liu, Y., Zhang, L., Khan, A., Wu, X., Wu, R., Wu, S., Huang, L., others, 2016. Probable hospital cluster of H7N9 influenza infection. N. Engl. J. Med. 374, 596–598. https://doi.org/10.1056/NEJMc1505359.
Fiers, M.W.E.J., Kleter, G.A., Nijland, H., Peijnenburg, A.A.C.M., Nap, J.P., Van Ham, R. C.H.J., 2004. AllermatchTM, a webtool for the prediction of potential allergenicity according to current FAO/WHO codex alimentarius guidelines. BMC Bioinform. 5, 1–6. https://doi.org/10.1186/1471-2105-5-133.
Galanis, K.A., Nastou, K.C., Papandreou, N.C., Petichakis, G.N., Pigis, D.G., Iconomidou, V.A., 2021. Linear B-cell epitope prediction for in silico vaccine design: a performance review of methods available via command-line interface. Int. J. Mol. Sci. 22, 3210. https://doi.org/10.3390/ijms22063210.
Gasteiger, E., Hoogland, C., Gattiker, A., Wilkins, M.R., Appel, R.D., Bairoch, A., others, 2005. Protein identification and analysis tools on the ExPASy server. Proteomics Protoc. Handb. 571–607. https://doi.org/10.1385/1-59259-890-0:571.
Gioia, C., Castilletti, C., Tempestilli, M., Piacentini, P., Bordi, L., Chiappini, R., Agrati, C., Squarcione, S., Ippolito, G., Puro, V., others, 2008. Cross-subtype immunity against avian influenza in persons recently vaccinated for influenza. Emerg. Infect. Dis. 14, 121. https://doi.org/10.1016/j.vetmic.2018.05.005.
Goodman, R.E., Ebisawa, M., Ferreira, F., Sampson, H.A., van Ree, R., Vieths, S., Baumert, J.L., Bohle, B., Lalithambika, S., Wise, J., others, 2016. AllergenOnline: a peer-reviewed, curated allergen database to assess novel food proteins for potential cross-reactivity. Mol. Nutr. Food Res. 60, 1183–1198. https://doi.org/10.1002/mnfr.201500769.
Grote, A., Hiller, K., Scheer, M., Münch, R., Nörtemann, B., Hempel, D.C., Jahn, D., 2005. JCat: a novel tool to adapt codon usage of a target gene to its potential expression host. Nucleic Acids Res. 33, W526–W531. https://doi.org/10.1093/nar/gki376.
Gupta, S.K., Deb, R., Dey, S., Chellappa, M.M., 2014. Toll-like receptor-based adjuvants: enhancing the immune response to vaccines against infectious diseases of chicken. Expert Rev. Vacc. 13, 909–925. https://doi.org/10.1586/14760584.2014.920236.
Hebditch, M., Carballo-Amador, M.A., Charonis, S., Curtis, R., Warwicker, J., 2017. Protein–Sol: a web tool for predicting protein solubility from sequence. Bioinformatics 33, 3098–3100. https://doi.org/10.1093/bioinformatics/btx345.
Horimoto, T., Kawaoka, Y., 2006. Strategies for developing vaccines against H5N1 influenza a viruses. Trends Mol. Med. 12, 506–514. https://doi.org/10.1016/J.MOLMED.2006.09.003.
Hui, D.S.C., 2008. Review of clinical symptoms and spectrum in humans with influenza A/H5N1 infection. Respirology 13, S10–S13. https://doi.org/10.1111/J.1440-1843.2008.01247.X.
Ilyushina, N.A., Bovin, N.V., Webster, R.G., 2012. Decreased neuraminidase activity is important for the adaptation of H5N1 influenza virus to human airway epithelium. J. Virol. 86, 4724–4733. https://doi.org/10.1128/JVI.06774-11/SUPPL_FILE/SUPPPLEMENTAL.DOCX.
Islam, M.S. Bin, Miah, M., Hossain, M.E., Kibria, K.M.K., 2020. A conserved multi-epitope-based vaccine designed by targeting hemagglutinin protein of highly pathogenic avian H5 influenza viruses. 3 Biotech 10, 1–16. https://doi.org/10.1007/s13205-020-02544-3.
Jespersen, M.C., Peters, B., Nielsen, M., Marcatili, P., 2017. BepiPred-2.0: improving sequence-based B-cell epitope prediction using conformational epitopes. Nucleic Acids Res. 45, W24–W29. https://doi.org/10.1093/NAR/GKX346.
Källberg, M., Margaryan, G., Wang, S., Ma, J., Xu, J., 2014. RaptorX server: a resource for template-based protein structure modeling. Methods Mol. Biol. 1137, 17–27. https://doi.org/10.1007/978-1-4939-0366-5_2.
Khan, M.T., Islam, R., Jerin, T.J., Mahmud, A., Khatun, S., Kobir, A., Islam, M.N., Akter, A., Mondal, S.I., 2021. Immunoinformatics and molecular dynamics approaches: next generation vaccine design against West Nile virus. PLoS One 16, e0253393. https://doi.org/10.1371/journal.pone.0253393.
Knutson, K.L., Schiffman, K., Disis, M.L., 2001. Immunization with a HER-2/neu helper peptide vaccine generates HER-2/neu CD8 T-cell immunity in cancer patients. J. Clin. Invest. 107, 477. https://doi.org/10.1172/JCI11752.
Koch, M., Camp, S., Collen, T., Avila, D., Salomonsen, J., Wallny, H.J., van Hateren, A., Hunt, L., Jacob, J.P., Johnston, F., Marston, D.A.A., Shaw, I., Dunbar, P.R., Cerundolo, V., Jones, E.Y., Kaufman, J., 2007. Structures of an MHC class I molecule from B21 chickens illustrate promiscuous peptide binding. Immunity 27, 885–899. https://doi.org/10.1016/J.IMMUNI.2007.11.007/ATTACHMENT/EBF06445-F9C9-4AD1-BA4A-CB3ED455944D/MMC1.PDF.
Kolaskar, A.S., Tongaonkar, P.C., 1990. A semi-empirical method for prediction of antigenic determinants on protein antigens. FEBS Lett. 276, 172–174. https://doi.org/10.1016/0014-5793(90)80535-Q.
Kozakov, D., Hall, D.R., Xia, B., Porter, K.A., Padhorny, D., Yueh, C., Beglov, D., Vajda, S., 2017. The ClusPro web server for protein–protein docking. Nat. Protoc. 12, 255–278. https://doi.org/10.1038/nprot.2016.169.
Kumar, A., Meldgaard, T.S., Bertholet, S., 2018. Novel platforms for the development of a universal influenza vaccine. Front. Immunol. 9, 600. https://doi.org/10.3389/FIMMU.2018.00600/BIBTEX.
Lafuente, E.M., Reche, P.A., 2009. Prediction of MHC-peptide binding: a systematic and comprehensive overview. Curr. Pharm. Des. 15, 3209–3220.
Lakadamyali, M., Rust, M.J., Zhuang, X., 2004. Endocytosis of influenza viruses. Microbes Infect. 6, 929–936. https://doi.org/10.1016/j.micinf.2004.05.002.
Larsen, M.V., Lundegaard, C., Lamberth, K., Buus, S., Lund, O., Nielsen, M., 2007. Large-scale validation of methods for cytotoxic T-lymphocyte epitope prediction. BMC Bioinform. 8, 1–12. https://doi.org/10.1186/1471-2105-8-424.
Lohia, N., Baranwal, M., 2017. Immune responses to highly conserved influenza A virus matrix 1 peptides. Microbiol. Immunol. 61, 225–231. https://doi.org/10.1111/1348-0421.12485.
López-Blanco, J.R., Aliaga, J.I., Quintana-Orti, E.S., Chacón, P., 2014. iMODS: internal coordinates normal mode analysis server. Nucleic Acids Res. 42, 271–276. https://doi.org/10.1093/nar/gku339.
Lpez, J.A., Weilenman, C., Audran, R., Roggero, M.A., Bonelo, A., Tiercy, J.M., Spertini, F., Corradin, G., 2001. A synthetic malaria vaccine elicits a potent CD8+ and CD4+ T lymphocyte immune response in humans. Implications for vaccination strategies. Eur. J. Immunol. 31, 1989–1998. https://doi.org/10.1002/1521-4141(200107)31:7<1989::AID-IMMU1989>3.0.CO;2-M.
Lundegaard, C., Lund, O., Nielsen, M., 2008. Accurate approximation method for prediction of class I MHC affinities for peptides of length 8, 10 and 11 using prediction tools trained on 9mers. Bioinformatics 24, 1397–1398. https://doi.org/10.1093/bioinformatics/btn128.
McAuley, J.L., Gilbertson, B.P., Trifkovic, S., Brown, L.E., McKimm-Breschkin, J.L., 2019. Influenza virus neuraminidase structure and functions. Front. Microbiol. 10, 39. https://doi.org/10.3389/fmicb.2019.00039.
McKeever, T.M., Lewis, S.A., Smith, C., Hubbard, R., 2011. Vaccination and allergic disease: a birth cohort study, 94, 985–989. https://doi.org/10.2105/AJPH.94.6.985.
Mohan, T., Verma, P., Nageswara Rao, D., 2013. Novel adjuvants & delivery vehicles for vaccines development: a road ahead. Indian J. Med. Res. 138, 779.
Mugunthan, S.P., Harish, M.C., 2021. Multi-epitope-based vaccine designed by targeting cytoadherence proteins of mycoplasma gallisepticum. ACS Omega 6, 13742–13755. https://doi.org/10.1021/acsomega.1c01032.
Pan, M., Gao, R., Lv, Q., Huang, S., Zhou, Z., Yang, L., Li, X., Zhao, X., Zou, X., Tong, W., Mao, S., Zou, S., Bo, H., Zhu, X., Liu, L., Yuan, H., Zhang, M., Wang, Daqing, Li, Z., Zhao, W., Ma, M., Li, Y., Li, T., Yang, H., Xu, J., Zhou, L., Zhou, X., Tang, W., Song, Y., Chen, T., Bai, T., Zhou, J., Wang, Dayan, Wu, G., Li, D., Feng, Z., Gao, G.F., Wang, Y., He, S., Shu, Y., 2016. Human infection with a novel, highly pathogenic avian influenza a (H5N6) virus: Virological and clinical findings. J. Inf. Secur. 72, 52–59. https://doi.org/10.1016/J.JINF.2015.06.009.
Peacock, T., Chain, B., 2021. Information-driven docking for TCR-pMHC complex prediction. Front. Immunol. 12 https://doi.org/10.3389/fimmu.2021.686127.
Peng, J., Xu, J., 2011. Raptorx: exploiting structure information for protein alignment by statistical inference. Proteins Struct. Funct. Bioinforma. 79, 161–171. https://doi.org/10.1002/PROT.23175.
Poland, G.A., Ovsyannikova, I.G., Jacobson, R.M., 2009. Application of Pharmacogenomics to Vaccines. https://doi.org/10.2217/pgs.09.25.
Rahman, N., Ali, F., Basharat, Z., Shehroz, M., Khan, M.K., Jeandet, P., Nepovimova, E., Kuca, K., Khan, H., 2020. Vaccine design from the ensemble of surface glycoprotein epitopes of SARS-CoV-2: an immunoinformatics approach. Vaccines 8, 423. https://doi.org/10.3390/vaccines8030423.
Rana, A., Akhter, Y., 2016. A multi-subunit based, thermodynamically stable model vaccine using combined immunoinformatics and protein structure based approach. Immunobiology 221, 544–557. https://doi.org/10.1016/j.imbio.2015.12.004.
Russell, R.J., Kerry, P.S., Stevens, D.J., Steinhauer, D.A., Martin, S.R., Gamblin, S.J., Skehel, J.J., 2008. Structure of influenza hemagglutinin in complex with an inhibitor of membrane fusion. Proc. Natl. Acad. Sci. 105, 17736–17741. https://doi.org/10.1073/PNAS.0807142105.
Saadi, M., Karkhah, A., Nouri, H.R., 2017. Development of a multi-epitope peptide vaccine inducing robust T cell responses against brucellosis using immunoinformatics based approaches. Infect. Genet. Evol. 51, 227–234. https://doi.org/10.1016/j.meegid.2017.04.009.
Saha, S., Raghava, G.P.S., 2006a. Prediction of continuous B-cell epitopes in an antigen using recurrent neural network. Proteins Struct. Funct. Bioinforma. 65, 40–48. https://doi.org/10.1002/prot.21078.

Saha, S., Raghava, G.P.S., 2006b. AlgPred: prediction of allergenic proteins and mapping of IgE epitopes. Nucleic Acids Res. 34, 202–209. https://doi.org/10.1093/nar/gkl343.

Shahsavandi, S., Ebrahimi, M.M., Sadeghi, K., Mahravani, H., 2015. Design of a heterosubtypic epitope-based peptide vaccine fused with hemokinin-1 against influenza viruses. Virol. Sin. 30, 200–207. https://doi.org/10.1007/s12250-014-3504-0.

Shrestha, B., Diamond, M.S., 2004. Role of CD8+ T cells in control of West Nile virus infection. J. Virol. 78, 8312–8321. https://doi.org/10.1128/JVI.78.15.8312-8321.2004.

Shtykova, E.V., Baratova, L.A., Fedorova, N.V., Radyukhin, V.A., Ksenofontov, A.L., Volkov, V.V., Shishkov, A.V., Dolgov, A.A., Shilova, L.A., Batishchev, O.V., Jeffries, C.M., Svergun, D.I., 2013. Structural analysis of influenza a virus matrix protein M1 and its self-assemblies at low pH. PLoS One 8, e82431. https://doi.org/10.1371/JOURNAL.PONE.0082431.

Singh, A., Thakur, M., Sharma, L.K., Chandra, K., 2020. Designing a multi-epitope peptide based vaccine against SARS-CoV-2. Sci. Rep. 10, 1–12. https://doi.org/10.1038/s41598-020-73371-y.

Solanki, V., Tiwari, V., 2018. Subtractive proteomics to identify novel drug targets and reverse vaccinology for the development of chimeric vaccine against Acinetobacter baumannii. Sci. Rep. 8, 1–19. https://doi.org/10.1038/s41598-018-26689-7.

Soltan, M.A., Elbassiouny, N., Gamal, H., Elkaeed, E.B., Eid, R.A., Eldeen, M.A., Al-Karmalawy, A.A., 2021. In silico prediction of a multitope vaccine against Moraxella catarrhalis: reverse vaccinology and Immunoinformatics. Vaccines 9, 669.

Su, S., Bi, Y., Wong, G., Gray, G.C., Gao, G.F., Li, S., 2015. Epidemiology, evolution, and recent outbreaks of avian influenza virus in China. J. Virol. 89, 8671–8676. https://doi.org/10.1128/JVI.01034-15 •.

Sun, H., Pu, J., Wei, Y., Sun, Y., Hu, J., Liu, L., Xu, G., Gao, W., Li, C., Zhang, X., others, 2016. Highly pathogenic avian influenza H5N6 viruses exhibit enhanced affinity for human type sialic acid receptor and in-contact transmission in model ferrets. J. Virol. 90, 6235–6243. https://doi.org/10.1128/JVI.00127-16.

Tabassum, R., Abbas, G., Azam, S.S., 2021. Immunoinformatics based designing and simulation of multi-epitope vaccine against multi-drug resistant Stenotrophomonas maltophilia. J. Mol. Liq. 340, 116899 https://doi.org/10.1016/j.molliq.2021.116899.

Terajima, M., Cruz, J., Leporati, A.M., Orphin, L., Babon, J.A.B., Co, M.D.T., Pazoles, P., Jameson, J., Ennis, F.A., 2008. Influenza a virus matrix protein 1-specific human CD8 + T-cell response induced in trivalent inactivated vaccine recipients. J. Virol. 82, 9283–9287. https://doi.org/10.1128/JVI.01047-08/ASSET/8A7E246E-1067-459D-B7D9-5E0D14B051B8/ASSETS/GRAPHIC/ZJV0180810220002.JPEG.

ul Qamar, M., Shokat, Z., Muneer, I., Ashfaq, U.A., Javed, H., Anwar, F., Bari, A., Zahid, B., Saari, N., 2020. Multiepitope-based subunit vaccine design and evaluation against respiratory syncytial virus using reverse vaccinology approach. Vaccines 8, 288. https://doi.org/10.3390/vaccines8020288.

Vajda, S., Yueh, C., Beglov, D., Bohnuud, T., Mottarella, S.E., Xia, B., Hall, D.R., Kozakov, D., 2017. New additions to the C lus P ro server motivated by CAPRI. Proteins Struct. Funct. Bioinforma. 85, 435–444. https://doi.org/10.1002/prot.25219.

Verma, S., Sugadev, R., Kumar, A., Chandna, S., Ganju, L., Bansal, A., 2018. Multi-epitope DnaK peptide vaccine against S. Typhi: an in silico approach. Vaccine 36, 4014–4022. https://doi.org/10.1016/j.vaccine.2018.05.106.

Wen, F., Yang, J., Guo, J., Wang, C., Cheng, Q., Tang, Z., Luo, K., Yuan, S., Huang, S., Li, Y., 2021. Genetic characterization of an H5N6 avian influenza virus with multiple origins from a chicken in southern China, October 2019. BMC Vet. Res. 17, 1–6. https://doi.org/10.1186/S12917-021-02903-Z/FIGURES/2.

WHO, W.H.O, 2018. World Health Organization Factsheet: Influenza (Seasonal) [WWW document]. URL. https://www.who.int/news-room/fact-sheets/detail/influenza-(seasonal).

Wiederstein, M., Sippl, M.J., 2007. ProSA-web: interactive web service for the recognition of errors in three-dimensional structures of proteins. Nucleic Acids Res. 35, 407–410. https://doi.org/10.1093/nar/gkm290.

Wu, C.-Y., Monie, A., Pang, X., Hung, C.-F., Wu, T.C., 2010. Improving therapeutic HPV peptide-based vaccine potency by enhancing CD4+ T help and dendritic cell activation. J. Biomed. Sci. 17, 1–10. https://doi.org/10.1186/1423-0127-17-88.

Wu, Z.-Q., Zhang, Y., Zhao, N., Yu, Z., Pan, H., Chan, T.-C., Zhang, Z.-R., Liu, S.-L., 2017. Comparative epidemiology of human fatal infections with novel, high (H5N6 and H5N1) and low (H7N9 and H9N2) pathogenicity avian influenza a viruses. Int. J. Environ. Res. Public Health 14, 263. https://doi.org/10.3390/ijerph14030263.

Yang, Z.-F., Mok, C.K.P., Peiris, J.S.M., Zhong, N.-S., 2015. Human infection with a novel avian influenza a(H5N6) virus. N. Engl. J. Med. 373, 487–489. https://doi.org/10.1056/NEJMC1502983/SUPPL_FILE/NEJMC1502983_DISCLOSURES.PDF.

Yousafi, Q., Amin, H., Bibi, S., Rafi, R., Khan, M.S., Ali, H., Masroor, A., 2021. Subtractive proteomics and Immuno-informatics approaches for multi-peptide vaccine prediction against Klebsiella oxytoca and validation through in silico expression. Int. J. Pept. Res. Ther. 27, 2685–2701. https://doi.org/10.1007/s10989-021-10283-z.

Zhang, Y., Shen, Z., Ma, C., Jiang, C., Feng, C., Shankar, N., Yang, P., Sun, W., Wang, Q., 2015. Cluster of human infections with avian influenza a (H7N9) cases: a temporal and spatial analysis. Int. J. Environ. Res. Public Health 12, 816–828. https://doi.org/10.3390/ijerph120100816.

Zheng, Y., Li, M., Wang, H., Liang, G., 2012. Japanese encephalitis and Japanese encephalitis virus in mainland China. Rev. Med. Virol. 22, 301–322. https://doi.org/10.1002/rmv.1710.